Journal of Theoretical Biology 462 (2019) 391–407

Contents lists available at ScienceDirect

Journal of Theoretical Biology

journal homepage: www.elsevier.com/locate/jtb

On the probabilistic nature of the species-area relation

Silvia Zaoli[a,1], Andrea Giometto[b,1], Jonathan Giezendanner[a], Amos Maritan[c], Andrea Rinaldo[a,d,*]

[a] Laboratory of Ecohydrology ECHO/IIE/ENAC/EPFL Ecole Polytechinque Fédérale de Lausanne, Lausanne, Switzerland
[b] Department of Physics, Harvard University, MA-02138 Cambridge MA, US
[c] Dipartimento di Fisica ed Astronomia, Università di Padova, and INFN, I-35131 Padova, Italy
[d] Dipartimento ICEA, Università di Padova, Padova, Italy

ARTICLE INFO

Article history:
Received 26 April 2018
Revised 16 November 2018
Accepted 27 November 2018
Available online 28 November 2018

Keywords:
Macroecology
Stochastic SARs
Neutral theory
Resource competition
Stochastic community dynamics

ABSTRACT

The Species–Area Relation (SAR), which describes the increase in the number of species S with increasing area A, is under intense scrutiny in contemporary ecology, in particular to probe its reliability in predicting the number of species going extinct as a direct result of habitat loss. Here, we focus on the island SAR, which is measured across a set of disjoint habitat patches, and we argue that the SAR portrays an average trend around which fluctuations are to be expected due to the stochasticity of community dynamics within the patches, external perturbations, and habitat heterogeneity across different patches. This probabilistic interpretation of the SAR, though already implicit in the theory of island biogeography and manifest in the scatter of data points in plots of empirical SAR curves, has not been investigated systematically from the theoretical point of view. Here, we show that the two main contributions to SAR fluctuations, which are due to community dynamics within the patches and to habitat heterogeneity between different patches, can be decoupled and analyzed independently. To investigate the community dynamics contribution to SAR fluctuations, we explore a suite of theoretical models of community dynamics where the number of species S inhabiting a patch emerges from diverse ecological and evolutionary processes, and we compare stationary predictions for the coefficient of variation of S, i.e. the fluctuations of S with respect to the mean. We find that different community dynamics models diverge radically in their predictions. In island biogeography and in neutral frameworks, where fluctuations are only driven by the stochasticity of diversification and extinction events, relative fluctuations decay when the mean increases. Computational evidence suggests that this result is robust in the presence of competition for space or resources. When species compete for finite resources, and mass is introduced as a trait determining species' birth, death and resource consumption rates based on empirical allometric scalings, relative fluctuations do not decay with increasing mean S due to the occasional introduction of new species with large resource demands causing mass extinctions in the community. Given this observation, we also investigate the contribution of external disturbance events to fluctuations of S in neutral community dynamics models and compare this scenario with the community dynamics in undisturbed non-neutral models. Habitat heterogeneity within a single patch, in the context of metapopulation models, causes variability in the number of coexisting species which proves negligible with respect to that caused by the stochasticity of the community dynamics. The second contribution to SAR fluctuations, which is due to habitat heterogeneity among different patches, introduces corrections to the coefficient of variation of S. Most importantly, inter-patches heterogeneity introduces a constant, lower bound on the relative fluctuations of S equal to the coefficient of variation of a habitat variable describing the heterogeneity among patches. Because heterogeneity across patches is inevitably present in natural ecosystems, we expect that the relative fluctuations of S always tend to a constant in the limit of large mean S or large patch area A, with contributions from community dynamics, inter-patches heterogeneity or both. We provide a theoretical framework for modelling these two contributions and we show that both can affect significantly the fluctuations of the SAR.

* Corresponding author.
E-mail address: andrea.rinaldo@epfl.ch (A. Rinaldo).
[1] These two authors contributed equally.

https://doi.org/10.1016/j.jtbi.2018.11.032

1. Introduction

Although natural ecosystems are often characterized by striking diversity of form and function, regularities emerge almost inevitably across scales of space, time and organizational complexity (Harte et al., 2009; Levin, 1992; Rybicki and Hanski, 2013). Such regularities are subsumed by macroecological 'laws' that describe statistical patterns in species' numbers, abundances and sizes (Banavar et al., 2007; Marquet et al., 2005; Zaoli et al., 2017). Arguably, the most important example of ecological 'law' is the Species–Area Relation (SAR). The SAR quantifies the observation that species richness S tends to increase with increasing sampling or patch area A, in a relationship firmly placed at the origins of quantitative ecology (Arrhenius, 1921; Gleason, 1922; MacArthur and Wilson, 1967). A distinction should be made between types of SARs under study, which radically differ in the way area and species sampling are chosen (Dengler, 2009; Drakare et al., 2006) thus reflecting different measures of biodiversity. Notably, the island SAR, which is the focus of this paper, is obtained by counting species inhabiting disjoint, isolated patches in the same biogeographical region (e.g. islands, lakes, mountain tops or any set of areas separated by environmental barriers, MacArthur and Wilson (1967)). This form of the SAR stems from the eco-evolutionary dynamics shaping communities on ecological and evolutionary timescales. The island SAR formulation most supported by empirical data (Triantis et al., 2012) states that the number of species S inhabiting a habitat patch increases as a power of its area, A, such that $S = cA^z$, where c is a constant and $z \leq 1$ is the SAR scaling exponent. SARs measured on adjacent, non-adjacent or nested patches (Dengler, 2009; Drakare et al., 2006) within a larger contiguous domain are not considered in this paper, and compared to island SARs they are affected by the spatial distribution of individuals (say, the degree of species clustering) within the domain and may not be best described by a power-law at all scales (Harte et al., 2009). One empirical discovery that is worth mentioning, but will not be directly addressed here, is that some SARs are not well described by a power law and may show different patterns in small islands versus larger ones, where *in situ* speciation is possible (see Losos and Schluter (2000), Wagner et al. (2014), Schluter and Pennell (2017) and references therein).

The interest in the SAR and in the value of its exponent has been broad from all of ecology, in particular for its implied predictive use to forecast the effects of large-scale environmental or climatic change on biodiversity (Thomas et al., 2004), in particular as a consequence of habitat loss or fragmentation (Borile et al., 2013; Durrett and Levin, 1996; Hanski et al., 2013). In fact, within a deterministic power-law framework, the fraction of species surviving a habitat reduction from an area A to A' would simply be equal to $(A'/A)^z$. Note that only the scaling exponent z matters for such a prediction (and not the proportionality constant), explaining the interest in the exponent's value, see e.g. Rybicki and Hanski (2013). Although such an estimate certainly neglects some important factors which have an impact on the number of surviving species, e.g. the spatial configuration of the remaining habitat (Rybicki and Hanski, 2013) and the temporal dynamics of extinctions (Pimm and Raven, 1995), the SAR still provides an order-of-magnitude estimate of species loss and can be used as a starting point to build more specific estimates. Against this background, assessing theoretically the nature of the SAR and the reliability of its predictions is an issue of longstanding interest to community ecology, biogeography, and macroecology.

Empirical island SAR curves typically display scatter around the mean trend and this scatter can have multiple origins. The first cause is measurement error, for example due to insufficient sampling effort missing rare species. Secondly, different environmental conditions on the disjoint patches included in the analysis could imply different proportionality constants c in the SAR $S = cA^z$ for each patch, producing a scatter in the plot of S vs A. The importance of this contribution to the observed scatter directly depends on the diversity of environmental conditions across the patches included in the analysis, e.g. their climate and resource availability. Finally, even in the absence of measurement error and for perfectly identical environmental conditions across patches, the number of species S has a residual noise due to the stochastic community dynamics within each patch (defined 'turnover noise' by Diamond and Gilpin (1980)). In models of community dynamics, the number of species S in stationary conditions results from the balance of competing stochastic processes, which according to neutral theory (Hubbell, 2001) are speciation, immigration and drift. Therefore, the number of species S should be seen as a stochastic variable subject to fluctuations. If we were able to measure the evolution of S with time within a patch, or compare it across exact replicates of the same patch with identical area A and in the absence of inter-patches habitat heterogeneity, S would assume different values according to its stationary distribution $p(S, t \to \infty|A) = p(S|A)$, where the symbol '$|A$' indicates the conditional probability given that patches have area A. The magnitude and relevance of these fluctuations in the observed scatter of the SAR can be investigated by means of stochastic models of community dynamics. However, past theoretical work (MacArthur and Wilson, 1963, 1967; Rosenzweig, 1995) focused mainly on the deterministic SAR emerging for the mean value of the number of species in patches of area A, $\langle S|A\rangle$, by determining its functional dependence on A and related coefficients (Azaele et al., 2016; Durrett and Levin, 1996; Lomolino, 2000), and studying its behavior following changes in speciation rate, typical dispersal length and patch size (Cencini et al., 2012; Pigolotti and Cencini, 2009; Shem-Tov et al., 2017). Much less attention has been devoted to determining and isolating the causes of scatter and to understanding to what extent such scatter might invalidate the significance of the observed SAR curve. One exception has been provided by Diamond and Gilpin (1980), who tackled the issue of the scaling of the relative fluctuations of S with patch area A in a model of the equilibrium theory of island biogeography (MacArthur and Wilson, 1967).

While the interest in studying average trends is not questionable, we argue that fluctuations of S may not be negligible with respect to their mean (Fig. 1) and thus they may be an important component of the SAR. Quantifying the effects of community dynamics stochasticity and inter-patches heterogeneity on the fluctuations of the SAR is a theoretically interesting problem. There would exist cases where, depending on the community dynamics within patches or the inter-patches heterogeneity, a particular value of S measured in field studies may differ significantly from its expected value across a set of disjoint patches or different measurement times. Mathematically, the magnitude of the relative fluctuations of the number of species S can be described via its coefficient of variation:

$$\mathrm{CV}(S) \equiv \frac{\sqrt{\langle S^2\rangle - \langle S\rangle^2}}{\langle S\rangle} = \frac{\sqrt{\mathrm{var}(S)}}{\langle S\rangle}. \tag{1}$$

When the relative fluctuations $\mathrm{CV}(S)$ decay with increasing $\langle S\rangle$, the random variable S can be considered essentially deterministic for collections of disjoint patches with large enough $\langle S\rangle$, because observable values lie within a negligible distance from the mean. In this work, we ask whether (and why) relative fluctuations may not decay with increasing $\langle S\rangle$. In such a scenario, when using a deterministic SAR one should be aware of its reduced predictive power due to the potential large distance of any single observation from

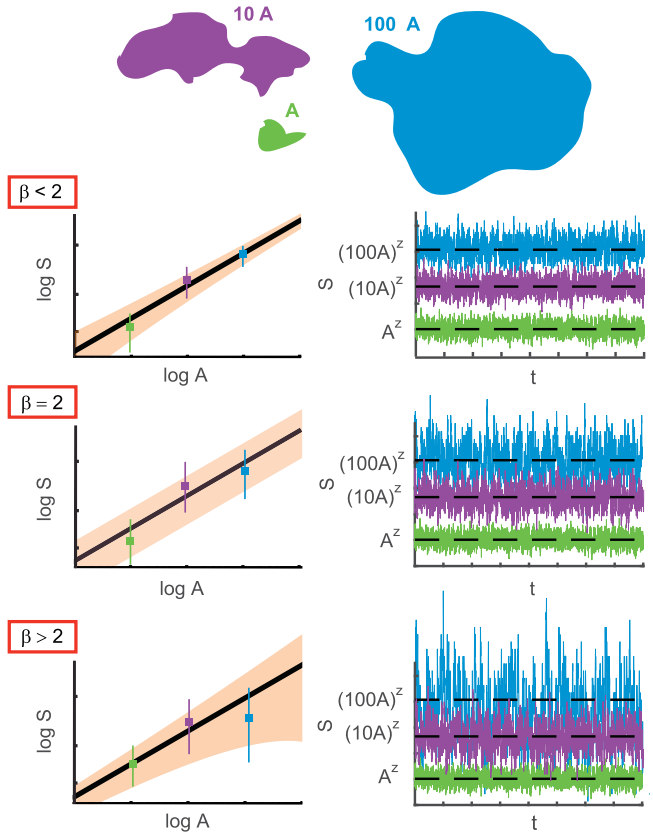

Fig. 1. A conceptual scheme highlighting the probabilistic structure of the SAR and the contribution of community dynamics to the fluctuations of S: (top panels) Three independent patches of area A, $10A$, 10^2A are sketched. The patches are meant to comply with the stipulations of the theory of island biogeography and we assume that there is no habitat heterogeneity among them; (lower panels) Three SAR scenarios are shown, differing for the value of the exponent β describing the scaling of the variance of S with the mean $\langle S\rangle$, i.e. $\mathrm{var}(S)\propto\langle S\rangle^{\beta}$. On the left, we plot the SAR prediction for the mean number of species with its confidence interval and an example of the outcome of a hypothetical measurement for each of the three areas. The plot, in double logarithmic scale, is based on a power-law SAR with slope equal to z, i.e. $\langle S|A\rangle = cA^z$. On the right, we plot examples of what a time-series of the measured number of species would look like in the three test patches, should a replicated field study be staged therein. From top to bottom, we considered the case of the Taylor's law exponent $\beta < 2$ in which relative fluctuations go to zero as A increases, the case $\beta = 2$ for which the variance scales with the mean and thus relative fluctuations are constant at all scales, and the case $\beta > 2$ for which relative fluctuations of S increase with A.

the average, depending of course on the value of $\mathrm{CV}(S)$. The scaling of the variance with the mean of positive random variables has been often found to conform to a power-law with exponent between 1 and 2, $\mathrm{var}(S)\propto\langle S\rangle^{\beta}$, an empirical observation that is often referred to as 'Taylor's law' or 'fluctuation scaling' (Cohen, 2014; Giometto et al., 2015; Taylor, 1961). This observation allows us to express the relative fluctuations of S, $\mathrm{CV}(S)$, in terms of the mean number of species $\langle S\rangle$, and the value of the exponent β determines the behavior of the relative fluctuations (Fig. 1):

$$\mathrm{CV}(S) \propto \langle S\rangle^{\beta/2-1}. \tag{2}$$

For $\beta < 2$, relative fluctuations decay with increasing $\langle S\rangle$, while for $\beta > 2$, relative fluctuations increase with increasing $\langle S\rangle$. For the exponent value $\beta = 2$, relative fluctuations are constant at all scales, i.e. for all values of $\langle S\rangle$. As an example, for a Poisson random variable X, $\mathrm{var}(X) = \langle X^2\rangle - \langle X\rangle^2 = \langle X\rangle$, therefore $\beta = 1$ and the relative fluctuations vanish in the limit $\langle X\rangle \to \infty$. On the other hand, for a random variable X distributed as a power-law with exponent $\alpha \in (1, 2)$, the sample mean and variance (Newman, 2005) yield $\beta = (3-\alpha)/(2-\alpha) \geq 2$, i.e. relative fluctuations are either constant or diverge in the $\langle X\rangle \to \infty$ limit, depending on the value of α. The value of β is therefore a useful quantity to characterize the fluctuations of S, and classify different models of community dynamics as done below.

In this work, we acknowledge that the number of species S inhabiting a patch of area A is a random variable with probability distribution $p(S|A)$ and thus we refer to the SAR as the relationship $\langle S|A\rangle = cA^z$. Note that the mean number of species $\langle S|A\rangle$ increases with the patch size A when $z > 0$, which is almost always found empirically, in particular for the island SAR. Therefore, when the relative fluctuations $\mathrm{CV}(S|A) \equiv \sqrt{\mathrm{var}(S|A)}/\langle S|A\rangle$ (here, $\mathrm{var}(S|A) \equiv \langle S^2|A\rangle - \langle S|A\rangle^2$) decay with increasing $\langle S|A\rangle$, we can equivalently state that they decay with increasing patch size A. Some of the community dynamics models considered in Section 2 do not model the patch size A explicitly, but are useful as starting points for our investigation. For those models, the probability distribution $p(S)$ and its cumulants are not conditional on A, and we study the behavior of relative fluctuations $\mathrm{CV}(S) \equiv \sqrt{\mathrm{var}(S)}/\langle S\rangle$ in the limit of large $\langle S\rangle$. We examine the statistics of S in a number of community dynamics models which include a diverse set of ecological processes and we characterize the scaling of the relative fluctuations of S with the mean. Exact results, which we review in Section 2.1, exist for the simplest models, i.e. the model of MacArthur and Wilson (1963, 1967) and the non-interacting neutral model, offering a natural starting point for the study of the behavior of fluctuations. We then show that species competition, under certain circumstances, can cause severe perturbations to the dynamics of S within a patch, leading to relative fluctuations of S which do not decay as the mean increases. Furthermore, we examine the effects of different types of external perturbations on the community inhabiting a patch, addressing the effects of their size and frequency in relation to patch size and recovery rate (due to speciation/immigration). The scope of such model comparison is to further our understanding of the possible statistical properties of S which we should expect in field observations of a single patch. Finally, we show that habitat heterogeneity across different patches causes an additional contribution to the relative fluctuations of S, which may dominate over the contribution due to community dynamics, or may be comparable in magnitude, depending on the community dynamics within the patches. Table 1 summarizes the results for the various community dynamics models considered.

2. Community dynamics contribution to SAR fluctuations

2.1. Species richness from minimalist models of community dynamics

We first consider a specific model of the equilibrium theory of island biogeography (MacArthur and Wilson, 1963) and review the results of Diamond and Gilpin (1980) on such model. In this model, the stationary number of species emerges from the balance between immigration from a species pool containing P species and extinction, with rates $I(S)$ and $E(S)$, respectively. In this approach, the variance of S is exactly (Diamond and Gilpin, 1980; MacArthur and Wilson, 1967):

$$\mathrm{var}(S) = \frac{I(\langle S\rangle)}{dE/dS - dI/dS}, \tag{3}$$

where the average number of species $\langle S\rangle$ is obtained from the condition:

$$I(\langle S\rangle) = E(\langle S\rangle). \tag{4}$$

Table 1
Summary of the community dynamics models investigated and their predictions for the exponent β describing how the relative fluctuations of S due to community dynamics scale with the average number of species.

Model	Relative fluctuations scaling
Poisson model (Section 2.1)	Relative fluctuations decay with the mean, $\mathrm{CV}(S) \propto \langle S \rangle^{-1/2}$
Mean-field multi-species voter model (Section 2.1)	Relative fluctuations decay with the mean, $\mathrm{CV}(S) \propto \langle S \rangle^{-1/2}$
Multi-species voter model (MSV, Section 2.2.1)	Relative fluctuations decay with the mean, $\mathrm{CV}(S) \propto \langle S \rangle^{-1/2}$
Neutral-spatially implicit model (N-SI, Section 2.2.2)	Relative fluctuations decay with the mean, $\mathrm{CV}(S) \propto \langle S \rangle^{-1/2}$
Non-neutral spatially implicit model with diversification rate independent of area (M1, Section 2.3)	Relative fluctuations are constant, $\mathrm{CV}(S) \propto 1$
Non-neutral spatially implicit model with diversification rate decreasing with area (M2, Section 2.3)	Relative fluctuations are constant, $\mathrm{CV}(S) \propto 1$
Neutral-spatially implicit model with external perturbations independent of S (N-SI-P1, Section 2.4)	Relative fluctuations decay with the mean, $\mathrm{CV}(S) \propto \langle S \rangle^{-1/2}$
Neutral-spatially implicit model with external perturbations proportional to S (N-SI-P2, Section 2.4)	For small areas relative fluctuations are constant, $\mathrm{CV}(S) \propto 1$
Metapopulation dynamics model (Section 2.5)	The variance decreases with the mean with a non-power-law pattern. Relative fluctuations decrease with the mean much faster than in all other models.

Diamond and Gilpin (1980) showed that, for a specific choice of $I(S)$ and $E(S)$, at stationarity $\mathrm{var}(S)$ increases linearly with $\langle S \rangle$ when $\langle S \rangle \ll P$, reaches a maximum around $\langle S \rangle = P/2$ and then decays to zero as $\langle S \rangle$ approaches P. Such result implies, therefore, that relative fluctuations decay as $1/\sqrt{\langle S \rangle}$ when $\langle S \rangle \ll P$ and even faster afterwards. This behavior is related to the lack of speciation in the model, limiting the maximum number of species to the number of species in the pool.

We can compare such predictions with the ones of a neutral model where new species are introduced by speciation and immigration without a fixed upper limit on S. Consider a community dynamics where new species appear as a point Poisson process with rate λ and are characterized by a birth rate b and a death rate d that are identical for all species, i.e. the model is neutral. For this model with non-interacting species, which we refer to as the *Poisson model*, the number of species S at stationarity is a Poisson random variable (Suweis et al., 2012) with mean:

$$\langle S \rangle = \lambda \langle \tau \rangle, \tag{5}$$

where $\langle \tau \rangle$ is the average lifetime of a species, also called persistence time (Appendix B). An alternative formulation of this model is the following: the arrival of new species in the community is a Poisson process of rate λ and their lifetimes τ are i.i.d. variables with mean $\langle \tau \rangle$. With this formulation, the fact that S is Poisson-distributed with mean given by Eq. (5) corresponds to a known result of queuing theory (Benes, 1965). As a consequence of $p(S)$ being a Poisson distribution, one has $\beta = 1$. Therefore, relative fluctuations decay with the mean and S is effectively deterministic in the limit of large S. The same result can be proved for the mean-field multi-species Voter model (Suweis et al., 2012) in patches of area A, where species interact through the competition for space, in the large A limit (when interactions become negligible). The Voter model is a spatially explicit stochastic model on a lattice (Clifford and Aidan, 1973; Durrett and Levin, 1996; Liggett, 1985), where each site is occupied by an individual characterized by its species. When an individual dies, it is replaced either by an individual of a new species (interpreted as a speciation event or immigration from outside the lattice) or by an offspring of another species present in the lattice (adjacent to the empty site in the nearest-neighbor version or from anywhere in the lattice in the well-mixed case). Note that, with the introduction of space, the mean lifetime $\langle \tau | A \rangle$ in a patch of size A becomes a function of A. For this model, Eq. (5) reads $\langle S|A \rangle = \lambda \langle \tau | A \rangle$, and provides a link between persistence times and the SAR (Bertuzzo et al. (2011), see also Appendix B).

The introduction of more realistic features such as a finite dispersal length, non-negligible interactions or the relaxation of the neutral assumption prevent exact results to be obtained for $p(S|A)$. In fact, interactions make persistence times τ not independent, while introducing a trait differentiating species, e.g. mass, makes the persistence times τ not identically distributed across species and the above results do not necessarily apply. Therefore, we explored numerically the statistical properties of S in a variety of stochastic models of community dynamics, varying the assumption of neutrality and the presence or absence of competition. We studied the stationary distributions $p(S|A)$ in different generalizations of the simple neutral model of non-interacting species presented above: we compared different mechanisms of competition for resources (Section 2.2), neutral and non-neutral models and different speciation mechanisms (Section 2.3). For each model and each of the simulated patch sizes A, we computed $p(S|A)$, its average $\langle S|A \rangle$, its variance $\mathrm{var}(S|A) \equiv \langle S^2|A \rangle - \langle S|A \rangle^2$ and the relative fluctuations $\mathrm{CV}(S|A)$. Furthermore, we computed $p(\tau|A)$ (i.e., the probability that a species in a patch of area A has a persistence time τ) and its average $\langle \tau|A \rangle$. In addition, we also explored the effect of intra-patch habitat heterogeneity by considering a metapopulation model (Rybicki and Hanski, 2013), where the biodiversity level is determined by the habitat diversity within the patch, allowing species with different niches to survive (Section 2.5). Also for this model, for each simulated patch size A, $p(S|A)$ was computed under randomization of the intra-patch landscape, along with its average, variance and relative fluctuations.

2.2. Neutral models with competition

We considered two different ways of introducing competition for a shared resource, i.e. interaction among species: a spatially explicit one in Section 2.2.1 and a spatially implicit one in Section 2.2.2.

2.2.1. Multi-species voter model (MSV)

First, we studied the Multi-Species Voter model (MSV) with speciation and nearest-neighbors dispersal. Here, each individual occupies a node of an $L \times L$ lattice (a patch of size $A = L^2$) and $N = L^2$ is the total number of individuals, therefore space is the common resource in this model. At each time step, one individual chosen at random dies and is replaced with probability λ by an individual of a new species and with probability $1 - \lambda$ by an offspring of one of its nearest neighbors. The probability λ should be interpreted as the sum of the probability of speciation and of the probability of immigration of a new species from outside the lattice, and will be called “diversification rate” hereafter. While for the well-mixed case (or equivalently for infinite dispersal length), in the limit $A \to \infty$, a parallel can be established with the non-interacting case (Suweis et al., 2012) allowing to extend the analytical results, no analytical results are known when the dispersal length is finite. A semi-analytical approach gives an approxima-

tion for $\langle S|A\rangle$ (Shem-Tov et al., 2017), but not for $p(S|A)$. The MSV model has been studied extensively in Bertuzzo et al. (2011), where the resulting species' persistence time distribution $p(\tau|A)$ was compared with the empirical one computed from presence/absence data of breeding birds. We simulated the MSV model on periodic lattices (patches) of size $A = L^2$ with $L = 50,\ 100,\ 200$ and diversification rate $\lambda = 10^{-3}$. We expect results to be robust with respect to the diversification rate λ. To compute $p(S|A)$ for the different areas, we obtained 1000 independent realizations of S at the stationary state for each value of A by simulating the model with the coalescent method (Etienne and Olff, 2004), which takes advantage of the dual representation of the Voter model (Holley and Liggett, 1975; Rosindell and Cornell, 2009; Rosindell et al., 2008). This method assures that the realizations of S are independent. Since persistence times cannot be measured with the coalescent method, we also performed one forward simulation of the model for each value of A. Species' persistence times were measured as the interval between the appearance of a species and its extinction. The simulations were continued until the estimate of $\langle\tau|A\rangle$ did not increase further with simulation length.

2.2.2. Neutral-spatially implicit model (N-SI)

Competition for resources can also be introduced in a spatially-implicit model, in which an A-dependent resource constraint is implemented in the birth and death rates. We consider here a neutral version of the community dynamics model introduced in Zaoli et al. (2017). Let A be the area of a patch, and let $\mathcal{R} \propto A$ be the resources supply rate. In the model, individual births and deaths are Poisson-distributed events, and an individual of a species with abundance n_i is born or dies with rates, respectively:

$$u_i(t) = n_i,$$
$$v_i(t) = \left[v_0 + (1 - v_0) r \frac{N(t)}{\mathcal{R}}\right] n_i, \tag{6}$$

where r is the resource consumption rate of an individual, $N(t)$ is the total number of individuals in the community at time t and the per-capita birth rate of an individual of unit mass is taken equal to one without loss of generality. We refrain from introducing a proportionality constant u_0 between u_i and n_i, which corresponds to re-scaling time by $1/u_0$. When the resource consumption of the community $rN(t)$ is equal to the resource supply rate $\mathcal{R}$, the birth rate is equal to the death rate, $u = v$, and the community has no net growth, but $N(t)$ will continue to fluctuate with time. Diversification is implemented as a Poisson process with constant rate λ. At each diversification event, a species is chosen at random and a random fraction of individuals from such species is assigned to a new species (this mode of speciation is analogous to what is frequently referred to as 'fission speciation'). In this model, space is introduced implicitly via the assumption $\mathcal{R} \propto A$, which determines the number of individuals that the patch can sustain. We simulated the model for $A = 10^i$ with $i = 2, 3, 4, 5$, $\lambda = 10^{-4}$, $v_0 = 1/2$ and $c = 10^{-4}$. Also in this case, we expect the results to be robust with respect to a broad range of parameters' variations. The stationary state was considered attained when the number of species S did not show a net change in time, but only fluctuations around a stationary mean value. To compute $p(S|A)$ at the stationary state, we sampled the number of species S with frequency $f = 10^{-5}$. Such a low sampling frequency guarantees the independence of the sampled values of S. Persistence times were measured as explained in Section 2.2.1. In the following, we will refer to this model as N-SI (Neutral-Spatially Implicit). Differently from the MSV model, where each individual always occupies one node, i.e. consumes a fixed amount of resources, here the neutral assumption for the resource consumption rate can be easily relaxed (see Section 2.3).

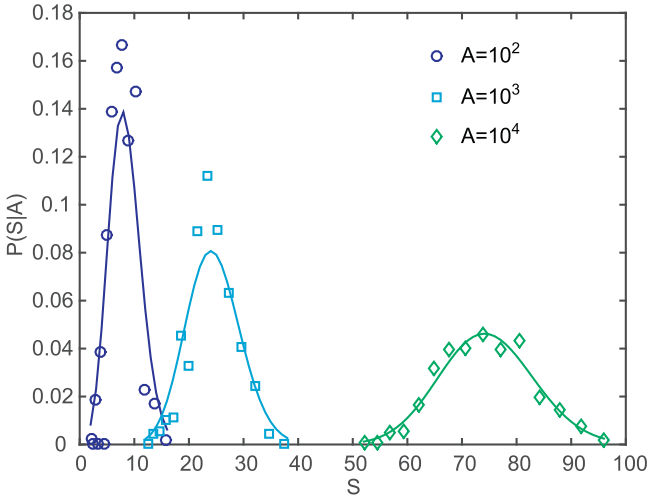

Fig. 2. $p(S|A)$ for the N-SI model. Colors refer to different values of A. Continuous lines are Poisson distributions with mean $\lambda\langle\tau|A\rangle$.

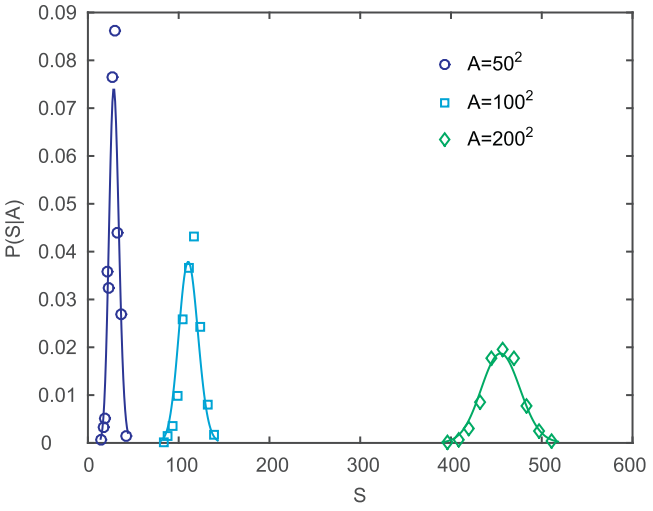

Fig. 3. Conditional probability distribution of the number of species S within a patch of area A. Here we show $p(S|A)$ for the MSV model with $\lambda = 10^{-3}$ and $A = L^2$ with $L = 50, 100, 200$ obtained from 1000 simulations of the model with the coalescent method. Continuous lines are Poisson distribution with mean $\lambda\langle\tau|A\rangle$, where $\langle\tau|A\rangle$ was obtained from a forward model simulation.

2.2.3. Comparison with the neutral model without competition

Numerical results suggest that the exact results valid in the non-interacting case (i.e., S being a Poisson variable with mean given by Eq. (5)) are still valid for the two models with competition in the large-area limit. Figs. 2 and 3 show $p(S|A)$ obtained from simulations of, respectively, the N-SI and MSV model for different values of A and the corresponding theoretical predictions for the non-interacting case, i.e. Poisson distributions with mean $\lambda\langle\tau|A\rangle$. The results match closely the predictions and, as expected for a Poisson random variable, $\mathrm{var}(S|A)$ scales as a power of $\langle S|A\rangle$ with an exponent β compatible with 1, i.e S is asymptotically deterministic. The estimates of β for the two models are, respectively $\beta = 0.985 \pm 0.005$ ($R^2 = 1.0$) and $\beta = 1.08 \pm 0.06$ ($R^2 = 0.99$). Fig. 4(a) displays the time-evolution of S for two different areas in the N-SI model (a similar dynamics is found for the MSV model). The average number of species is found to scale as a power-law of A. The values of z estimated by linear least squares fitting of $(\log A, \log S)$ for the MSV and N-SI models are, respectively, $z = 0.998 \pm 0.002$

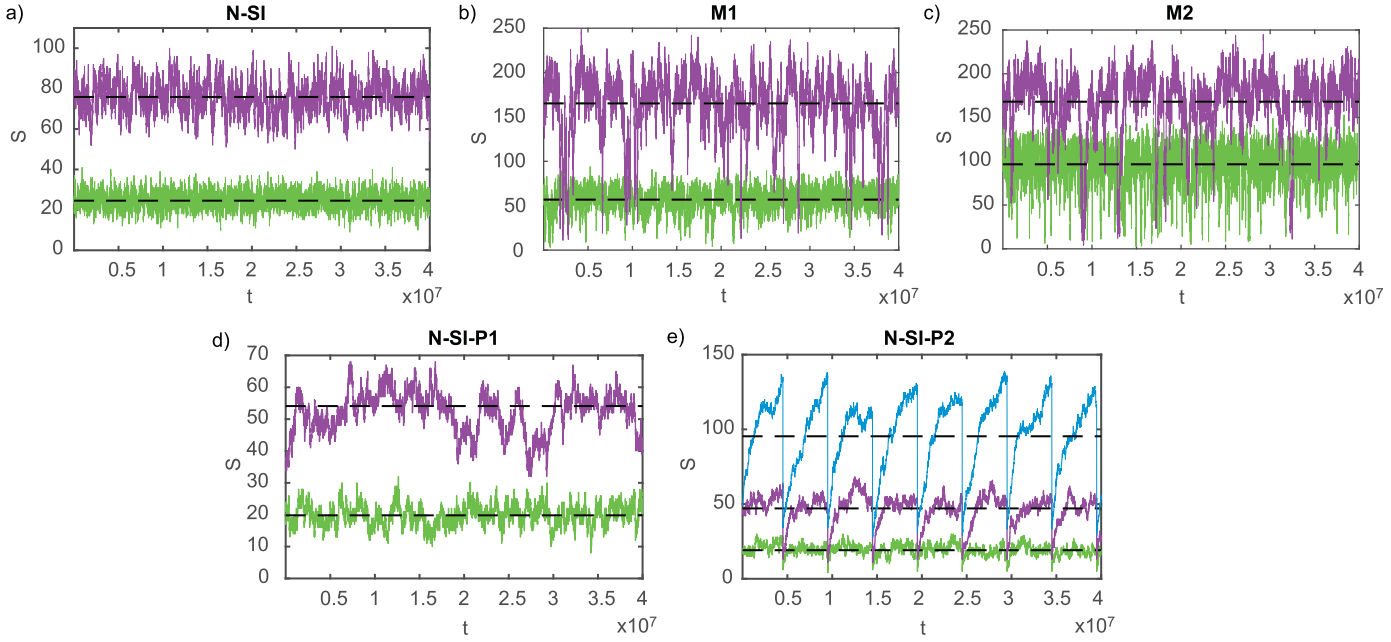

Fig. 4. Dynamics of the number of species S in the models presented in the main text. a) Model N-SI with $\lambda = 10^{-4}$, areas 10^3 (green) and 10^4 (purple); b) model M1 with $\lambda = 10^{-2}$, areas 10^3 (green) and 10^4 (purple); c) model M2 with $\lambda = A^{-0.5}$, areas 10^3 (green) and 10^4 (purple); d) model N-SI-P1 with $\lambda = 10^{-4}$, areas 10^3 (green) and 10^4 (purple); e) model N-SI-P2 with $\lambda = 10^{-4}$, areas 10^3 (green), 10^4 (purple) and 10^5 (blue). Note that the decrease in the number of species at fixed frequencies is due to the specific perturbations that we added by design to the neutral dynamics (see text). Black dotted lines mark the average S. The metapopulation dynamics model is not shown because we don't solve for its temporal dynamics to compute the statistics of S. (For interpretation of the references to colour in this figure legend, the reader is referred to the web version of this article.)

($R^2 = 1.0$) and $z = 0.496 \pm 0.001$ ($R^2 = 0.99$). Note that the value $z = 1$ for the MSV model is expected from the results of Shem-Tov et al. (2017) to hold independently of λ. Some considerations regarding the distribution of persistence times in the two models are presented in Appendix B.

2.3. Non-neutral models

The assumption of neutral dynamics, which neglects differences in species traits such as vital rates, is often employed in ecological modeling because analytic results can often be derived and compared to empirical measurements (Azaele et al., 2016), often with good levels of accuracy. Not distinguishing different species by characteristic traits such as body size, however, prevents the comparison between theoretical models and empirical patterns that are related to such traits, for example scale-invariant community size spectra (Marañón, 2015), the power-law relationship between the typical body mass of a species and its average abundance (Damuth, 1981), and others (Zaoli et al., 2017). To reproduce these patterns in community dynamics models, we recently showed in Zaoli et al. (2017) that different species must be distinguished by their characteristic body size and the scaling of vital (Brown et al., 2004) and resource consumption (Kleiber, 1932) rates with body size needs to be accounted for. In these community dynamics models, the dependence of physiological rates on body mass explains the observed difference in the success (in terms of abundance) of species with different body sizes. These results suggest that individual body mass, which is a key biological trait affecting a species' physiology and ecology (Brown et al., 2004; Giometto et al., 2013; Kleiber, 1932; Marañón, 2015), is also fundamental for the emergence of widespread ecological patterns in natural ecosystems. In this section, we investigate the dynamics and relative fluctuations of S in variants of the community dynamics models introduced in Zaoli et al. (2017), which are generalizations of the model N-SI to the non-neutral case. In these models, an individual of a species with abundance n_i and body mass m_i is born or dies with rates, respectively:

$$u_i = n_i m_i^{-1/4},$$
$$v_i = \left[v_0 + (1 - v_0) r \frac{\sum_j n_j m_j^{3/4}}{\mathcal{R}} \right] n_i m_i^{-1/4}, \tag{7}$$

where r is the resource consumption rate of an individual with unit mass and the per-capita birth rate for an individual of unit mass is taken equal to one without loss of generality. The exponent values $-1/4$ and $-3/4$ are the typical values for the corresponding allometries and it was shown (Zaoli et al., 2017) that they affect the scaling exponents of macroecological patterns, but not their functional form and covariations. Similarly to the corresponding neutral model (N-SI), the community net growth rate is zero when the community consumes all the available resources, i.e. when $r \sum_j n_j m_j^{3/4} = \mathcal{R} \propto A$. The two variants that we investigated here differ in the diversification mechanism: in model M1, diversification is implemented as a Poisson process with constant rate λ. In model M2, the overall rate of diversification λ depends on the area of the patch as $\lambda(A) = \lambda_0 A^{-\xi}$. This choice accounts for the finding of Bertuzzo et al. (2011), which showed that the species diversification rate scales with the area as $\lambda \propto A^{-\xi}$ with $\xi = 0.84$. This result agrees with the interpretation of λ as the sum of the rate of immigration and that of speciation, as the arrival of new species by immigration is expected to diminish as the patch area increases (Chisholm and Lichstein (2009), Appendix A).

In models M1 and M2, diversification is implemented via a fission mechanism as in model N-SI. The mass m_j of the descendant species j is obtained as $m_j = \max\{m_0; k \cdot m_i\}$, where k is a positive random number extracted from a lognormal distribution with mean and variance equal to one. The maximum in the expression for m_j introduces a bound on the minimum mass m_0 that a species can attain (Zaoli et al., 2017). The mass of the parent species is left unchanged. The distribution of species' masses in the patch is determined by the combination of this multiplica-

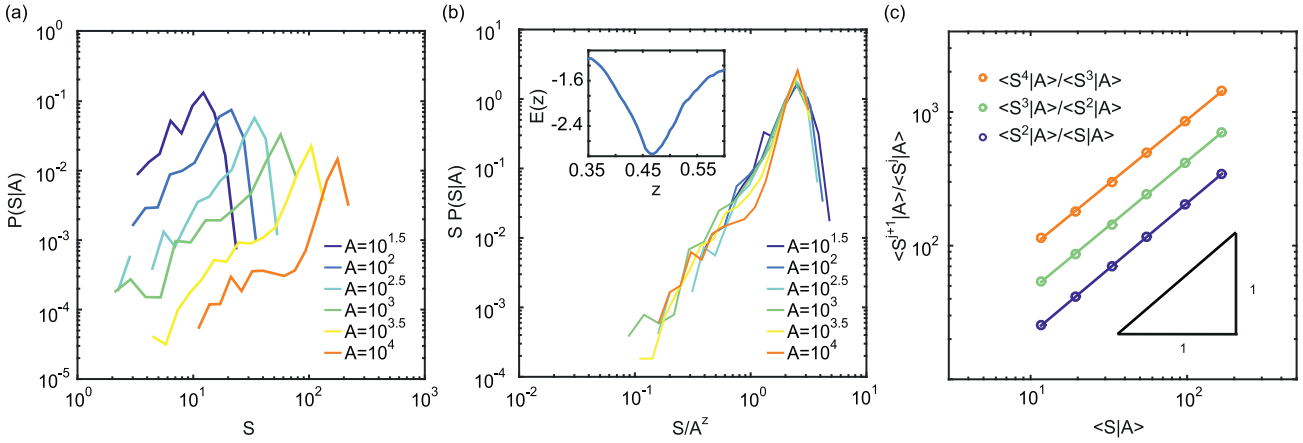

Fig. 5. Statistics of S for model M1. (a) $p(S|A)$, different colors refer to different values of $A = 10^i$, from $i = 1.5$ to $i = 4$. (b) Collapse of $p(S|A)$. Eq. (8) of the main text is verified because $Sp(S|A)$ versus S/A^z collapse on the same curve for different values of A. Inset: the minimum of the functional $E(z)$ provides the best estimate for the exponent and the associated error (Bhattacharjee and Seno, 2001). (c) Scaling of the ratio of consecutive moments with $\langle S \rangle$.

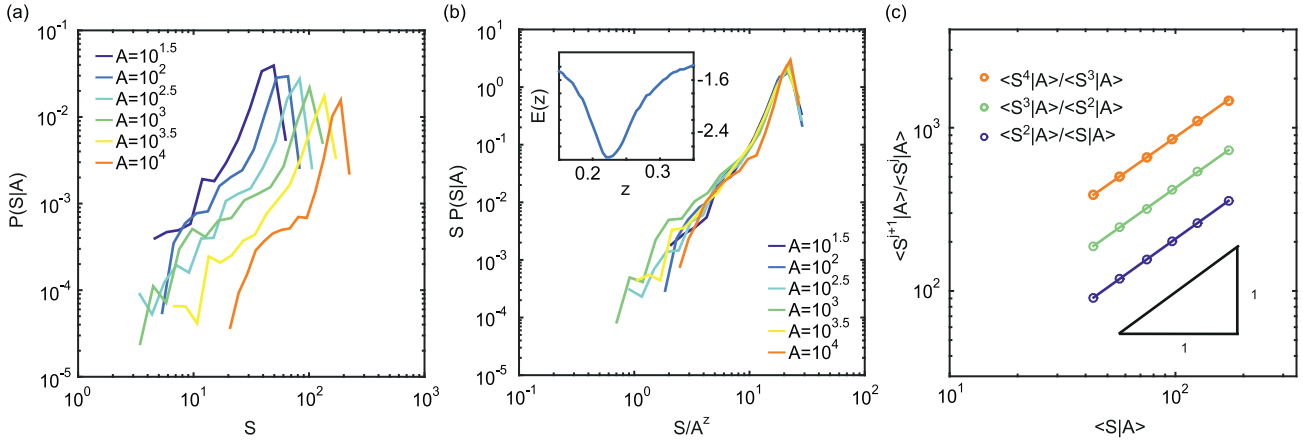

Fig. 6. Statistics of S for model M2. (a) $p(S|A)$, different colors refer to different values of $A = 10^i$, from $i = 1.5$ to $i = 4$. (b) Collapse of $p(S|A)$. Eq. (8) is verified because $Sp(S|A)$ versus S/A^z collapse on the same curve for different values of A. Inset: the minimum of the functional $E(z)$ provides the best estimate for the exponent and the associated error (Bhattacharjee and Seno, 2001). (c) Scaling of the ratio of consecutive moments with $\langle S \rangle$.

tive bounded process, known to produce power-laws (Didier and Rama, 1997; Solomon and Levy, 1996), and the birth/death dynamics. We note here that models M1 and M2 differ from the community dynamics model studied in Zaoli et al. (2017) because here we don't impose the constraint that the total metabolic rate should remain unchanged before and after a diversification event. We lift this constraint here because the diversification event may correspond to the immigration of a species with high resource consumption rate, which may cause the community to temporarily consume more resources than the resource supply rate $\mathcal{R}$. When this occurs, species' abundances rapidly decline to bring the community back to an overall consumption rate equal to $\mathcal{R}$. Imposing the constraint would therefore restrain the fluctuations which we want to study. We simulated models M1 and M2 for $A = 10^i$ with $i = 1.5, 2, 2.5, 3, 3.5, 4$ and parameters values $c = 10^{-3}$, $m_0 = 1$. The diversification rate was set to $\lambda = 10^{-2}$ for M1, while for M2 we used $\lambda_0 = 1$ and $\xi = 0.5$. The number of species and the persistence times were measured as for the N-SI model.

The dynamics of the random variable S in the two models, displayed in Fig. 4(b) and (c), shows strikingly different features in comparison with the neutral model. In particular, the coefficient of variation $\mathrm{CV}(S|A) \propto \langle S|A \rangle^{\beta/2-1}$ does not decrease with A, i.e. $\beta \simeq 2$. The species' number distributions, shown in Figs. 5(a) and 6(a), deviate strongly from a Poisson distribution, with fluctuations quantified, respectively, by $\beta = 1.88 \pm 0.05$ (M1) and $\beta = 1.93 \pm 0.14$ (M2). Rather than being Poisson distributed, species number distributions in models M1 and M2 are described by the following finite-size scaling form (Giometto et al., 2013):

$$p(S|A) = \frac{1}{S}\,\mathcal{F}\left(\frac{S}{cA^z}\right), \tag{8}$$

where $\mathcal{F}$ is a function such that $\mathcal{F}(x) \to 0$ for $x \to 0, \infty$ and c describes the quality of the habitat, which we will assume to be constant for this section. Eq. (8) accounts for the fact that in an ecosystem of area A, like in many other complex systems, there is an emerging scale for the number of species, S, that diverges as cA^z. This suggests that the probability distribution of S, instead of depending on both A and S separately, depends only on the dimensionless ratio $S/(cA^z)$. The pre-factor, $1/S$, is there for dimensional reason since $\int p(S|A)dS$ has to be a pure number, i.e. $p(S|A)$ must have the dimension of $1/S$. The validity of Eq. (8) is shown by data collapse (Bhattacharjee and Seno, 2001; Giometto et al., 2013), which consists in plotting the curves $Sp(S|A)$ versus S/A^z for different values of A and showing that curves computed with different values of A collapse, as shown in Figs. 5(b) and 6(b). Note that an attempt to collapse the distributions obtained with the N-SI model according to Eq. (8) fails (Fig. 7), due to the different behavior of the fluctuations of S in neutral and non-neutral community dynamics models. To visually highlight the difference be-

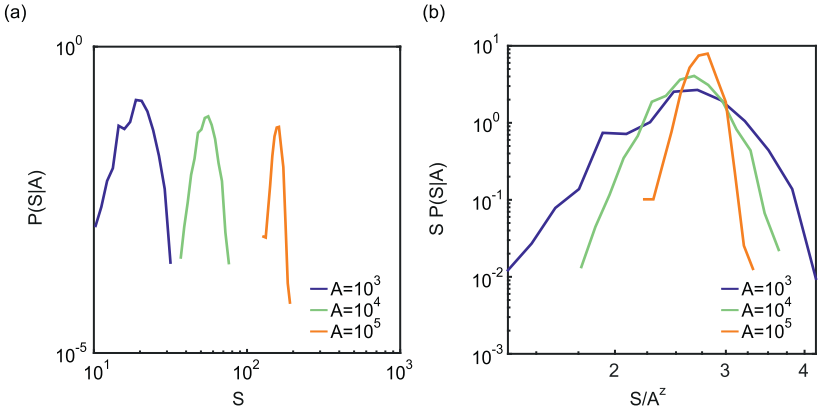

Fig. 7. Failure of the collapse in Eq. (8) of the main text for the N-SI model. (a) $p(S|A)$ (log-log scale). Colors refer to different values of A. (b) Attempt to collapse the distributions as suggested by Eq. (8) of the main text. The failure of the collapse shows that, in the neutral models, the fluctuations behave in a remarkably different way than in the non-neutral models.

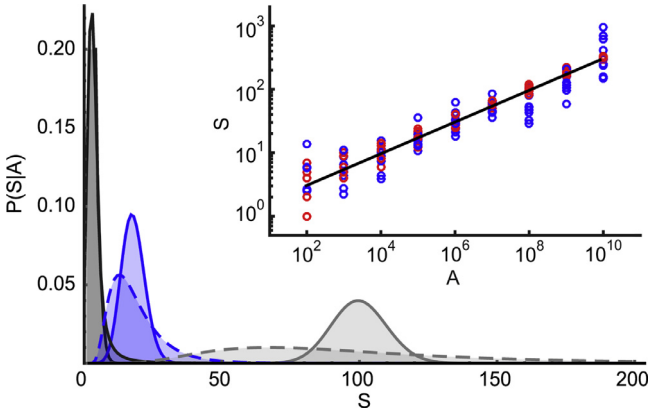

Fig. 8. Comparison of Poisson distributions (continuous lines) and lognormal distributions (dashed lines) with means A^z, namely with $z = 1/4$ and $A = 10^2$ (black), 10^5 (blue) and 10^8 (grey). The lognormal distribution satisfies Eq. (8) with $F(x) = 1/\sqrt{2\pi\sigma^2}e^{-(\log(x)-\mu)^2/(2\sigma^2)}$. To have $\langle S|A\rangle = A^z$, we set $\mu = -\sigma^2/2$. We set the parameter σ such that the variance of the lognormal for $A = 10^2$ is equal to the variance of the Poisson distribution for $A = 10^2$ (but not for larger or smaller areas, otherwise the lognormal distribution would not satisfy Eq. 8). Inset: values of S extracted from a Poisson distribution (red) and from a lognormal distribution (blue) with mean A^z, with $z = 1/4$ and $A = 10^i$ for $i = 2, \ldots, 10$. The parameter σ of the lognormal distribution was set as explained above. For each value of the area, 10 extracted values are shown. The black line is $S = cA^z$. (For interpretation of the references to colour in this figure legend, the reader is referred to the web version of this article.)

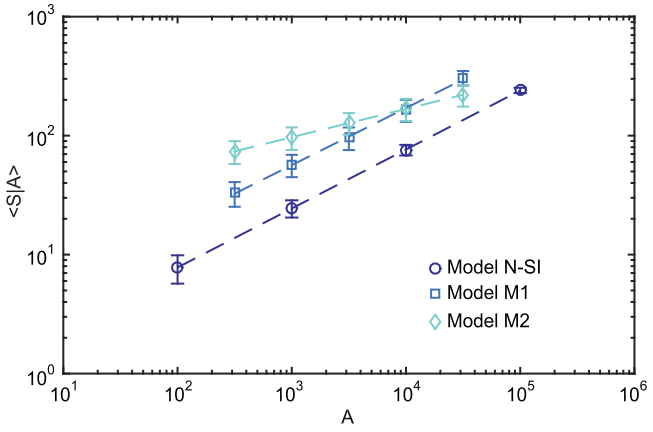

Fig. 9. Scaling of the average number of species $\langle S|A\rangle$ vs the patch size A for models N-SI (circles), M1 (squares) and M2 (diamonds). Lines are least square fit of log-transformed data, see text for exponent estimates. Error bars are SEM.

tween distributions that satisfy Eq. (8) and the Poisson distribution, we plot in Fig. 8 a lognormal distribution that satisfies Eq. (8) and a Poisson distribution with the same mean and the same variance at a small value of the patch area A. Because of the scaling properties of $p(S|A)$ with A implied by Eq. (8), the variance of the two distributions is only identical at such small value of A. Accordingly, Fig. 8 shows that the distribution of the form in Eq. (8) spreads out much faster than the Poisson distribution as the patch area A is increased, showing that fluctuations of S are much larger for the former class of distributions. The effect of the different behavior of fluctuations of S on the uncertainty of hypothetical field measurements is exemplified in the inset of Fig. 8, which compares the scattering of single values of S around the $S = cA^z$ line in a (A, S) plot for values distributed according to Eq. (8) and according to a Poisson distribution. The values of z yielding the best collapses for M1 and M2, computed with the algorithm of Bhattacharjee and Seno (2001), are, respectively, $z = 0.46$ with 95% confidence interval [0.44, 0.52], and $z = 0.222$ with 95% confidence interval [0.216, 0.244]. A consequence of the validity of Eq. (8) (see Appendix C) is that $\langle S|A\rangle \propto A^z$ (Fig. 9). We verified that the values of the exponent z estimated by performing a least-squares linear fit of the pairs $(\log A, \log\langle S|A\rangle)$ are compatible with the values obtained by the collapse of the distributions. The least-squares linear fit estimates of z in models M1 and M2 are, respectively: $z = 0.464 \pm 0.001$, and $z = 0.233 \pm 0.002$. Eq. (5) proves still valid: Figs. B.14(c) and B.15(c) in Appendix B show the points $(\lambda(A)\langle\tau|A\rangle, \langle S|A\rangle)$ for different values of A falling on the 1:1 line. As expected from Eq. (8) (see Appendix C), consecutive moments of $p(S|A)$ satisfy $\langle S^{j+1}|A\rangle/\langle S^j|A\rangle \propto \langle S|A\rangle$ (see Figs. 5(c) and 6(c)). Therefore, $\mathrm{var}(S|A) = \langle S^2|A\rangle - \langle S|A\rangle^2 \propto \langle S|A\rangle^2$, i.e. $\beta = 2$. Using Eq. (2), this implies that the relative fluctuations of S remain constant as the patch area A grows, i.e. $\mathrm{CV}(S) = \text{constant}$ at any value of $\langle S\rangle$ and A. As a consequence, for the two non-neutral models M1 and M2 it is not possible to define a threshold area above which the deviation of S from the deterministic prediction is smaller than any prescribed value. Note, however, that for practical purposes the constant value of the relative fluctuations $\mathrm{CV}(S)$ may be sufficiently small to treat S as an effectively-deterministic variable.

We speculate that the reason for the different scaling of the relative fluctuations of S with respect to $\langle S\rangle$ between the neutral and the non-neutral community dynamics models lies in the different characteristics of the perturbations to the community caused by diversification events. In the neutral case, the appearance or disap-

pearance of a species causes a fixed change in the available resources (and therefore in the death rates) because each species has the same consumption rate (or occupies the same space, in the case of the MSV model). When A increases (and so does $\mathcal{R}$), this change becomes relatively smaller and so do the relative fluctuations around stationary mean values. In the non-neutral models investigated here, instead, the appearance or disappearance of a species brings a change in the total resource consumption rate which depends on its mass. As A increases, the patch can sustain larger and larger species, therefore the potential amplitude of fluctuations increases with A. These observation motivated us to investigate how the presence and magnitude of external perturbations can influence the relative fluctuations of S. In Section 2.4 we examine the dynamics of neutral models in which external perturbations are imposed to the community in order to disentangle their effect from the diversification mechanism, and to better understand how external perturbations affect the stationary probability distribution of the number of species S.

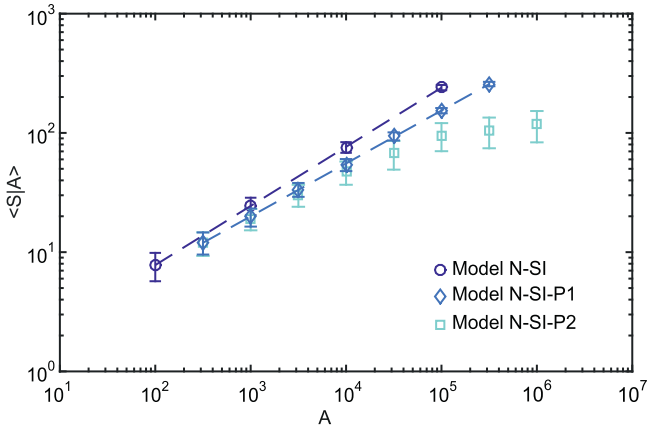

Fig. 10. Scaling of the average number of species $\langle S|A\rangle$ versus patch size A in models N-SI (circles), N-SI-P1 (diamonds) and N-SI-P2 (squares). Lines are least square fit of log-transformed data, see text for exponent estimates. Error bars are SEM.

2.4. Role of external perturbations

In Section 2.3, we hypothesized that perturbations are the most important factor in determining the temporal fluctuations of S within a single habitat patch, and in particular that the dependence of their amplitude on the patch area A is key to discriminate between the two limiting behaviors found for the relative fluctuations of S in the limit of large $\langle S\rangle$. In the two non-neutral models M1 and M2, perturbations arise naturally from the diversification dynamics, where a new species entering the community by speciation or immigration would increase resource consumption and therefore determine a resource debt causing extinctions, i.e. downward fluctuations of S. Recovery from perturbations, on the other hand, is controlled by the diversification rate. In models M1 and M2, the rate at which perturbations happen is related to the recovery rate, rendering the exploration of their interplay impossible. Also, it is not possible to control the size of such perturbations *a priori*. In general, however, the rates of perturbation and diversification may be unrelated, for example when perturbations are caused by the environment. In this section, we examine the effect of imposing external perturbations of a given size and frequency, which can be controlled independently from the diversification rate. Here, we have chosen to assign a constant frequency of perturbations that does not vary with the patch area A, to assess the effect of perturbations of equal magnitude and frequency on patches of different areas. The N-SI community dynamics is an appropriate model to study the effect of external perturbations on the community, as the fluctuations of S in the N-SI model vanish in the limit of large $\langle S\rangle$.

Perturbations may have different sources, e.g. climatic or environmental events or temporary shifts in resource availability. As such, they vary in frequency and in the way in which they affect habitat patches. Here, we model the effect of transient disturbances directly in terms of species loss. For simplicity, we assume that disturbances occur with a fixed frequency, but expect equivalent results if they occur as a Poisson process. We compare two types of perturbations. In model N-SI-P1, we add perturbations of fixed magnitude to the dynamics of model N-SI, regardless of S: with a fixed frequency ν_p, a fixed number of species S_p is removed from the community. In model N-SI-P2, instead, perturbations grow with the number of species S in the patch: with a fixed frequency ν_p, a fraction f_p of species is removed from the community. This second type of perturbation could describe, for example, responses to environmental change: imagine that each species has a certain probability q to survive, adapting to the new environmental conditions; then, on average $(1-q)S$ species will go extinct. We simulated the two models for $A = 10^i$ with $i = 2.5, 3, 3.5, 4, 4.5, 5, 5.5$, $S_p = 5$, $f_p = 3/4$ and $1/\nu_p = 5\cdot 10^6$. Fig. 4(d) and (e) display the temporal dynamics of S in the two cases. As expected, the statistics of S in model N-SI-P1 do not differ strongly from the unperturbed case, yielding $\beta = 0.96 \pm 0.07$ ($R^2 = 0.975$). Relative fluctuations therefore vanish rather fast with increasing patch size. The SAR shows a power-law pattern with a slope comparable with the value of z measured in the unperturbed case (Fig. 10), $z = 0.436 \pm 0.005$ ($R^2 = 0.99$). The dynamics of model N-SI-P2, shown in Fig. 4(e), is instead rather different. For small areas, between two perturbations the community is able to return to the stationary state of the unperturbed model, with Poisson fluctuations around the mean value of S. Although $\beta \simeq 2$ and thus CV(S) is constant, i.e. relative fluctuations do not decay in the limit of large $\langle S\rangle$, if the patch is observed at timescales that are smaller than the perturbation timescale $1/\nu_p$ one would see no differences with respect to the unperturbed case. However, increasing the area causes the recovery time to increase, and the community will spend less and less time in the stationary state corresponding to the unperturbed patch, until a threshold value of A is reached, above which the community is unable to ever reach the unperturbed stationary state. When this situation occurs, the observed value of S might be far from the average corresponding to the stationary undisturbed community even at small timescales, and strongly dependent on the history of perturbations. The patch area at which this behavior starts depends on the interplay of diversification rate and perturbation rate. This non-stationary regime shows deviations from a pure power-law both in the SAR (Fig. 10), whose slope decreases gradually towards zero, and in Taylor's law. The decreasing slope of the SAR is qualitatively explained by a simplified deterministic description of the model dynamics, where S grows linearly in time with rate s with a hard limit at $\bar{S}_{stat} = cA^z$ (corresponding to the stationary average of S in the unperturbed model N-SI) and a perturbation occurring with rate ν_p makes fS species go extinct, where S is the number of species when the perturbation occurs. As shown in Appendix D, one can distinguish between two cases: when $\eta = \nu_p f cA^z/s \leq 1$ the unperturbed stationary value $\bar{S}_{stat}$ is reached, while when $\eta > 1$ it is never reached. One can show (see Appendix D) that the slope of the scaling of $\langle S|A\rangle$ with increasing A is z when $\eta \ll 1$, but decreases as η increases, reaching zero when $\eta \geq 1$. For Taylor's law, a value of $\beta = 3$ is predicted at small η values, decreasing with increasing η. Taylor's law in model N-SI-P2 indeed shows a slope $\beta \sim 3$ for intermediate areas, but the decrease is not seen at the simulated areas. This simple model identifies the factors playing a role in determining the dynamics of biodiversity in the presence of perturbations.

When the size of perturbations increases with S (as in model N-SI-P2), the quantity $\eta = \nu_p f c A^z/s$ determines whether the community spends most of the time in its unperturbed stationary state (small η) or whether it spends most or all the time recovering from perturbations ($\eta \geq 1$). In particular, all the other factors being fixed, a larger community will spend more time recovering, as is seen clearly in Fig. 4(e). This differs from the case in which perturbation size and diversification rate are independent of patch size, as in model N-SI-P1, in which patches of all sizes have the same behavior: either they all return to the stationary state, or no one does.

2.5. Effect of intra-patch habitat heterogeneity in a metapopulation dynamics model

Within a given patch, the availability of different niches might change in time, affecting the number of species surviving in it and therefore creating additional variability. We studied a spatially-explicit metapopulation model, a well-established tool to study biodiversity patterns in a spatially-heterogeneous environment (Bertuzzo et al., 2015; Grilli et al., 2015; Hanski and Ovaskainen, 2000; Rybicki and Hanski, 2013) which allows us to assess the contribution of intra-patch habitat heterogeneity to the fluctuations of S. The metapopulation model originally proposed in Hanski (1998) describes a metapopulation composed of subpopulations of a single species inhabiting different sites of a hetereogeneous landscape. The model does not include interaction among species, therefore species survival is only driven by the heterogeneous characteristics of the landscape. Rybicki and Hanski (2013) have shown that, considering metapopulations of several different species with different niches, such metapopulation model is a highly meaningful metacommunity model if the strengths of the species competition remain relatively weak. The metapopulation model is based on the interplay between extinction and colonization dynamics. Each species has a probability p_i to be present (with one or more individuals) in a site i of the landscape (patch), which is a $L \times L$ lattice of area $A = L^2$. Species do not interact and thus they have independent dynamics. Let E_i be the rate at which a species becomes extinct in site i and C_i the rate at which the site is colonized. The probability of occupancy p_i of site i is then governed by

$$\frac{dp_i}{dt} = C_i(1 - p_i) - E_i p_i. \tag{9}$$

Each site is characterized by a habitat type, determined by the value of a parameter h, $0 \leq h \leq 1$. A species is characterized by 5 parameters: the colonization rate c, the extinction rate e, the phenotype ϕ, the niche width γ and the average dispersal distance $1/\alpha$. For a focal species, the fitness in a site i with habitat parameter h_i is $q = \exp\left[-(h_i - \phi)^2/(2\gamma^2)\right]$. The fitness, which is larger when ϕ is similar to h_i, determines how well the species will perform in that site, i.e. the probability that it will become extinct, the extinction rate being defined as $E_i = e/q_i$. In turn, the colonization rate, given by $C_i = c/(2\pi)\sum_{j\neq i}\alpha^2 e^{-d_{ij}\alpha} q_j p_j$, governs the interactions between the different sites. Species parameters are extracted at random from a uniform distribution in a suitable interval. The values of h characterizing the landscape are also extracted at random, but with a fixed spatial correlation (see below for details) and are constant in time. It was shown (Hanski and Ovaskainen, 2000) that the condition under which Eq. (9) has an equilibrium solution different from $p_i = 0\ \forall i$ is:

$$\lambda_M > e/c, \tag{10}$$

where λ_M is the metapopulation capacity, i.e. the leading eigenvalue of an appropriate matrix, which depends on the landscape and on the species phenotype ϕ, niche width γ and dispersal range $1/\alpha$. It is therefore said that a species is persistent in the landscape if it satisfies the condition in Eq. (10). To study the variability in the number of species persisting in a patch of a given size in the presence of intra-patch habitat heterogeneity, we considered a pool of $S_0 = 500$ species, evaluated how many satisfied the condition in Eq. (10) and repeated the evaluation in a set of 1000 different random landscapes at fixed spatial correlation with the same pool of species. Spatially correlated random landscapes were generated with two alternative methods. The first is the one used in Rybicki and Hanski (2013), while the second uses the HYDRO_GEN algorithm (Bellin and Rubin, 1996) for the generation of correlated random fields, which has the advantage of allowing us to set a prescribed correlation. We considered the landscape areas $A = 25^2,\ 50^2,\ 100^2,\ 200^2$. We initially generated 1000 landscapes of size 200^2, then obtained the 1000 smaller landscapes as subsets. Species parameter ranges were: $c \in [0.25, 2]$, $e \in [0.025, 0.4]$, $\phi \in [0.1, 0.9]$, $\gamma \in [0.1, 0.5]$, $\alpha \in [0.07, 1]$. To increase the species pool without increasing the computational time (which is mainly dependent on the λ_M computation), for each of the 500 sets of ϕ, γ and λ we extracted 15 additional values of c and e, effectively enlarging the species pool to $S_0 = 8000$.

This model differs from the ones presented in the previous sections in that the number of persisting species is not determined by the equilibrium of the competing stochastic processes of speciation and extinction, but to the diversity of habitat types present within a patch. A larger patch tends to have more habitat diversity, therefore more species (on average) are able to persist in it. The $p(S|A)$ resulting from the metapopulation model with the two different methods of landscape generation are shown in Figs. 11(a) and (b). The variance decreases with the mean with a pattern that is not described by a power-law, and therefore an estimation of β is not possible. However, relative fluctuations decrease with the average much faster than in all other considered models, at least as $1/\langle S|A\rangle$. Note that by using the condition in Eq. (10) to count the number of surviving species, we are effectively averaging over the stochasticity of the dynamics in each individual patch. Therefore, the observed variability is only that due to the intra-patch habitat heterogeneity. We can therefore conclude that the variability generated by intra-patch habitat heterogeneity at fixed spatial correlation is negligible with respect to the one possibly caused by community dynamics, at least within the assumptions of this model.

3. Contribution of inter-patches habitat heterogeneity to SAR fluctuations

In this section, we consider the contribution of inter-patches habitat heterogeneity to the relative fluctuations of the number of species S. We assume that the patches over which the species-area relationship is measured differ in a habitat variable c (e.g., the resource supply rate) that takes values in $[0, \infty)$ and has distribution $p(c|A)$ across patches of area A. Within a patch with habitat variable c and area A, we assume that the mean number of species S, computed over time, scales linearly with c, i.e. $\langle S|A,\ c\rangle \equiv \Sigma_S S p(S|A,\ c) \propto c$, where the symbol '$|c$' denotes the temporal mean computed within a patch with habitat variable c. The coefficient of variation of S across patches of area A is given by:

$$\mathrm{CV}(S|A) \equiv \frac{\sqrt{\mathrm{var}(S|A)}}{\langle S|A\rangle} = \sqrt{\frac{\int_0^\infty dc\ p(c|A)\langle S^2|A,c\rangle}{\left[\int_0^\infty dc\ p(c)\langle S|A,c\rangle\right]^2} - 1}, \tag{11}$$

which depends on how the community dynamics within patches of area A and habitat variable c affect the moments $\langle S|A,\ c\rangle$ and $\langle S^2|A,\ c\rangle$, and on the distribution of the habitat variable, $p(c|A)$. We can use Eq. (11) and the results of the previous sections to compute the relative fluctuations of S assuming different community dynamics within each patch. The results derived in the previous sections give

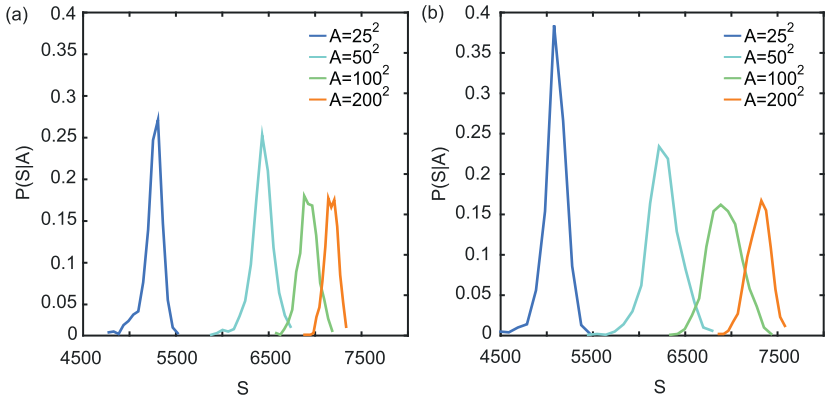

Fig. 11. $p(S|A)$ for the metapopulation model with landscapes generated according to Rybicki and Hanski (2013) (a) and with the HYDRO_GEN algorithm (see text) (b). Colors, from blue to orange, refer to landscape sizes $A = 25^2, 50^2, 100^2, 200^2$. (For interpretation of the references to colour in this figure legend, the reader is referred to the web version of this article.)

us $\langle S|A, c\rangle$, as shown in the following subsections for two classes of community dynamics models. For models in which space is not modeled explicitly, the distributions of S and c and their cumulants are not conditional on A, as seen in the next subsection.

3.1. Poisson model with implicit space

We consider here the neutral model that we discussed in Section 2.1, in which new species are introduced by speciation and immigration with rate λ and species are neutral with birth and death rates b and d, respectively. In this model, the mean number of species is equal to $-\lambda/b \log(1-b/d) = -\gamma \log(1-x)$, where we defined $\gamma = \lambda/b$ and $x = b/d$ for ease of notation. Our assumption that $\langle S|c\rangle \propto c$ can be satisfied if we assume that the diversification rate λ is proportional to c, i.e. $\lambda(c) = c\lambda$. With these assumptions, the distribution of species numbers within a patch with habitat variable c is given by:

$$p(S|c) = (1-x)^{c\gamma} \frac{[-c\gamma \log(1-x)]^S}{S!}, \tag{12}$$

and thus:

$$\langle S|c\rangle \equiv \sum_S S p(S|c) = -c\gamma \log(1-x), \tag{13}$$

$$\langle S^2|c\rangle \equiv \sum_S S^2 p(S|c) = -c\gamma \log(1-x) + c^2\gamma^2[\log(1-x)]^2 = \langle S|c\rangle + \langle S|c\rangle^2. \tag{14}$$

We find, for the relative fluctuations of S:

$$\mathrm{CV}(S) \equiv \sqrt{\frac{1}{\langle S\rangle} + \frac{\mathrm{var}(c)}{\langle c\rangle^2}} \xrightarrow{\langle S\rangle \to \infty} \sqrt{\frac{\mathrm{var}(c)}{\langle c\rangle^2}} \equiv \mathrm{CV}(c). \tag{15}$$

For a given distribution of the habitat variable $p(c)$ with finite mean and variance, $\mathrm{var}(c)/\langle c\rangle^2$ is a constant, and so the relative fluctuations of S don't go to zero in the limit of large $\langle S\rangle$ as the fluctuations caused by the community dynamics do within each patch (Section 2.1). Instead, relative fluctuations tend to the relative fluctuations of the habitat variable c.

3.2. Non-neutral models

In Section 2.3, we found that the distribution of species numbers in the non-neutral models M1 and M2 satisfies the scaling form given in Eq. (8). Note that the distribution in Eq. (8) satisfies our assumption that the mean number of species within a patch with habitat variable c scales linearly with c, i.e. $\langle S|A, c\rangle = cA^z$, because:

$$\langle S^j|A, c\rangle = c^j A^{jz} q_j, \tag{16}$$

with $q_j \equiv \int_0^\infty dx\ x^{j-1}\mathcal{F}(x)$ (to satisfy $\langle S|A, c\rangle = cA^z$, $\mathcal{F}$ is rescaled such that $q_1 = 1$). The relative fluctuations of S within a patch of area A and habitat variable c, caused by the stochastic community dynamics within the patch, are thus given by:

$$\mathrm{CV}(S|A, c) \equiv \frac{\sqrt{\mathrm{var}(S|A, c)}}{\langle S|A, c\rangle} = \sqrt{\frac{q_2}{q_1^2} - 1} \equiv \mathrm{CV}_{cd}(S), \tag{17}$$

which is a constant independent of A and c and the subscript cd stands for 'community dynamics'. The relative fluctuations of S across all patches are given by:

$$\mathrm{CV}(S|A) \equiv \frac{\sqrt{\mathrm{var}(S|A)}}{\langle S|A\rangle} = \sqrt{\frac{q_2}{q_1^2}\frac{\langle c^2|A\rangle}{\langle c|A\rangle^2} - 1} = \sqrt{[\mathrm{CV}_{cd}(S)^2 + 1][\mathrm{CV}(c|A)^2 + 1] - 1}, \tag{18}$$

which is an expression that accounts for both the community dynamics contribution to the relative fluctuations of S (which is identical for any choice of A and c) and the contribution due to inter-patches habitat heterogeneity.

4. Discussion

When the SAR is used to predict biodiversity and biodiversity responses to habitat loss or fragmentation, it is implicitly assumed that the average value of S in patches of area A, $\langle S|A\rangle$, described by the SAR is representative of what could be actually measured empirically, and that all ecosystem features of interest are stationary. Our work characterizes the fluctuations of S theoretically and highlights the contribution of fluctuations due to the stochastic nature of the community dynamics within patches and the contribution of habitat heterogeneity across the patches over which the SAR is measured.

Neglecting habitat heterogeneity between different patches, when relative fluctuations of $\langle S\rangle$ due to the stochastic community dynamics decay with increasing mean S (or, equivalently, increasing patch size A), they eventually become negligible in a large-enough patch (Fig. 1). Nevertheless, fluctuations might still be important for small patches. When relative fluctuations do not decay (or decay very slowly), patches of any size maintain the same relative level of stochasticity. If this level is non-negligible, the predictions of the SAR will not be representative of the behavior of individual patches, for which S may fall far apart from the predicted

average. Our results are based on an extensive survey of models of community dynamics reflecting different assumptions on the ecological dynamics within a habitat patch and external perturbations that affect it. The scaling behavior of the relative fluctuations of S in the different models is summarized in Table 1. Our analysis, while encompassing only some of the many possible models of community dynamics, shows that different models can lead to very different predictions for the fluctuations of the number of species S due to the community dynamics within a patch. We show that such fluctuations do not have a universal behavior but rather depend on the main ecological processes reflected in various model assumptions. Specifically:

- In a neutral framework where fluctuations are only driven by the stochasticity of diversification and of extinction events, biodiversity is asymptotically deterministic, i.e. its relative fluctuations decay with increasing patch size. Fluctuations are non-negligible only for small areas, where single measurements of S may deviate significantly from the deterministic prediction $S = cA^z$. It is possible to define a threshold area above which the expected deviation of S from $\langle S|A\rangle$ is smaller than a fixed threshold ϵ_t. More precisely, if $\langle S|A\rangle = cA^z$ is the deterministic prediction, then:

$$\mathrm{CV}(S|A) = \frac{1}{\sqrt{\langle S|A\rangle}} = \frac{1}{\sqrt{cA^z}} \leq \epsilon_t \iff A \geq \left(\frac{1}{\epsilon_t\sqrt{c}}\right)^{2/z}.$$

  We produced computational evidence that this result is also valid in the presence of competition for space or resources, a case in which the analytic results valid for the non-interacting case still prove applicable;
- The introduction of mass as a trait determining the resource consumption of individuals (Brown et al., 2004; Zaoli et al., 2017) can cause large fluctuations in the number of species due to the occasional introduction by speciation/immigration of new species with large resource consumption rate. The over-exploitation of the patch resources following such events triggers mass extinctions. The related stationary distribution $p(S|A)$ displays relative fluctuations which remain constant as the patch area A increases ($\beta = 2$, i.e. constant $\mathrm{CV}(S)$). Note that non-neutral resource consumption does not necessarily cause this behavior of the fluctuations. In fact, as found in Zaoli et al. (2017), if the introduction of new species in the community (by immigration or speciation) is strictly constrained by supply limitation, i.e. the total community consumption rate can never exceed the supply rate, fluctuations behave similarly to the neutral case and the distribution of S does not satisfy Eq. (8).
- Peaks in resource consumption caused by the arrival of new species are one possible cause of fluctuations for non-neutral community dynamics models within a patch. We explored the effect of fixed-frequency, external perturbations on the dynamics of biodiversity in neutral community dynamics models and found that such effect depends on the specific properties of the perturbations. Perturbations whose magnitude does not scale with the number of species lead to relative fluctuations of S that vanish in the limit of large patch size. Instead, when the magnitude of perturbations increases with the number of species, larger communities need progressively longer times to recover and the stationary unperturbed state is progressively less informative about the state of the community at any given time. Depending on the ratio between the frequency of perturbations and the recovery rate, on the perturbations intensity and on the patch size, the community can still be considered stationary at short timescales and far from perturbation events, and the conclusions found for the unperturbed neutral dynamics apply.
- Habitat heterogeneity within a single patch, e.g. as introduced by Rybicki and Hanski (2013), causes small variability in the number of coexisting species which decays relatively fast with the patch area. The contribution of intra-patch habitat heterogeneity to the fluctuations of S is thus negligible with respect to the fluctuations caused by the stochasticity of community dynamics or inter-patches heterogeneity.

We hope that our investigation of the magnitude of relative fluctuations in various community dynamics models will encourage further empirical measurements of the magnitude of relative, temporal fluctuations of S in patches subject to emigration, immigration and disturbance processes. Our investigation of relative fluctuations of S in a suite of community dynamics models provides a set of null expectations for what might be measured empirically. Ideally, empirical measurements would be done in patches of different areas with similar environmental conditions (e.g., similar climate), in order to minimize the contribution to SAR fluctuations due to habitat heterogeneity among different patches. To measure temporal fluctuations in each of these patches, long-term times series of species numbers are required (Dornelas et al., 2014; Vellend et al., 2013). These long-term time series would also prove useful to spot trends highlighting non-stationarity, a situation for which further theoretical work is required. For example, Vellend et al. (2013) and Dornelas et al. (2014) provide meta-analyses of various time-series with durations up to several decades. While overall there is no dominating trend, a number of single time series show an increasing or decreasing trend, signaling non-stationarity (Dornelas et al., 2014). Moreover, through repeated observations in time, recovery dynamics after a perturbation may be assessed, say, after a fire or the arrival of an invasive species. Identifying the time required to return to stationarity after perturbation and comparing it to the expected time between consecutive perturbation events would allow assessing whether S should be expected to spend most of its time around its stationary unperturbed average, or else in transient states possibly far from it. The study of the dynamics following a perturbation would also indicate whether its effects scale with patch size, which would allow discriminating between the scenarios of model N-SI-P1 and N-SI-P2. One could, for example, observe whether the arrival of an invasive species causes more extinctions in a more diverse community than in a less diverse one.

Accounting for habitat heterogeneity among different patches, we find that the relative fluctuations of S tend to a constant in the limit of large $\langle S|A\rangle$, irrespective of whether the relative fluctuations of S due to the community dynamics within single patches tend to zero or are constant at all scales. If the relative fluctuations of S due to the community dynamics within single patches tend to zero in the limit of large $\langle S|A\rangle$, the relative fluctuations of S across different patches tend to the coefficient of variation of the habitat variable c. If the relative fluctuations of S due to the community dynamics within single patches are constant at all scales, instead, the relative fluctuations of S across different patches are also constant at all scales, and their constant value combines both the community dynamics and the habitat heterogeneity contributions. Therefore, because habitat heterogeneity inevitably characterizes collections of islands or disjoint patches in the natural environment, we find that the relative fluctuations of S are always constant, and do not scale with $\langle S|A\rangle$ or A. Equivalently, the standard deviation of S scales linearly with $\langle S|A\rangle$, and in a log-log plot of single measurements of S versus A this would correspond to a constant scatter of S values around the SAR $\langle S|A\rangle = cA^z$ for any value of A. The constant value of $\mathrm{CV}(S)$ determines the amplitude of such a scatter, and according to such value the fluctuations of the SAR may or may not need to be addressed when using the SAR in practice.

5. Statement of authorship

SZ, AG, AM and AR designed the study. SZ and AG performed the analyses. JG implemented the metapopulation models. JG, AM and AR assisted with the analyses. SZ, AG, JG, AM and AR wrote the manuscript.

Acknowledgments

Funds from the Swiss National Science Foundation Projects 200021_157174, P2ELP2_168498 and P400PB_180823 and from the Horizon 2020 ECOPOTENTIAL Project 641762 are gratefully acknowledged. We thank Enrico Bertuzzo for useful discussions.

Appendix A. Speciation rate dependence on *A*

Losos and Schluter (2000) found that the per-species speciation rate is smaller in small island than in large ones, and that in islands larger than a certain threshold the speciation rate increases with island area. A per-species speciation rate increasing with area implies a total speciation rate increasing with area even faster. Eq. (5), satisfied by the neutral models and by models M1 and M2, quantifies the effect of a dependence of the speciation rate on A on the SAR slope. From Eq. (5) it follows that if the speciation rate is defined piecewise (constant for islands below a threshold area and increasing with area above threshold) the SAR will also have two different slopes before and after the threshold area, as observed by Losos and Schluter (2000). In our model M2, a speciation rate decreasing with A allowed us to find a realistic value of z ($z \simeq 1/4$). A speciation rate increasing with area, as the one suggested for larger islands, would produce a SAR with $z > 1/2$. This might be in agreement with the data shown in Fig. 3 of Losos and Schluter (2000), where large islands display a SAR slope $z = 0.76$.

Appendix B. Persistence time distributions

The persistence time distributions of the analyzed community dynamics models, as shown in Figs. B.12, B.13, B.14(a) and (b) and B.15(a) and (b), satisfy the following relation:

$$p(\tau|A) = \frac{1}{A^\theta} G\left(\frac{\tau}{A^\theta}\right) \tag{B.1}$$

with $\theta = z$ for models MSV, N-SI and M1 and $\theta = z + \xi$ for model M2, where z is the exponent of the SAR. The function $G(x)$ is such that $G(x) \sim c$ when $x < 1$, with $c > 0$ a constant and $\lim_{x\to\infty} G(x) = 0$. This result is in agreement with Eq. (5), in fact, when A is large:

$$\begin{aligned}\langle \tau|A\rangle &= \int_1^\infty \tau\, p(\tau|A) d\tau = \frac{1}{A^\theta}\int_1^\infty \tau G\left(\frac{\tau}{A^\theta}\right) d\tau = A^\theta \int_{1/A^\theta}^\infty x G(x) dx \\ &\approx A^\theta \left[c\int_{1/A^\theta}^1 x dx + \int_1^\infty x G(x) dx \right] \\ &= A^\theta \left[\frac{c}{2} A^{-2\theta} + c' \right] \propto A^\theta \end{aligned} \tag{B.2}$$

where $x = \tau/A^z$, $c' > 0$ is a constant and we used the properties of $G(x)$ to evaluate the integrals. Therefore, substituting in Eq. (5) of the main text and recalling that for M2 one has $\lambda(A) = \lambda_0 A^{-\xi}$, we find $\langle S|A\rangle \propto A^z$.

In the MSV model, a more precise characterization of $p(\tau|A)$ is possible. In fact, as found in Bertuzzo et al. (2011), the distribution of persistence times $p(\tau|A)$ is a power-law with exponential cutoff when $\tau > A$, where A is the number of time-steps in a 'generation', i.e. the time interval when on average every individual dies and gets replaces. For $\tau < A$, $p(\tau)$ is roughly constant (Fig. B.13). Therefore, we can write:

$$p(\tau|A) = \mathcal{C} \begin{cases} 1 & \text{for } \tau \le A \\ \left(\frac{\tau}{A}\right)^{-\alpha} e^{-\lambda(\tau/A - 1)} & \text{for } \tau > A \end{cases} \tag{B.3}$$

where $\mathcal{C} = \left[A + A^\alpha e^\lambda \left(\frac{\lambda}{A}\right)^{\alpha-1} \Gamma(1-\alpha, \lambda) \right]^{-1}$ is the normalization constant. The value of α depends on the topology of the lattice (dimension and connectivity, see Bertuzzo et al. (2011)). For the 2D lattice considered here, a maximum likelihood fit of the tail of the distribution to a power-law with exponential cutoff gives $\alpha \sim 3/2$. The fitted curves are the dashed lines in Fig. B.13.

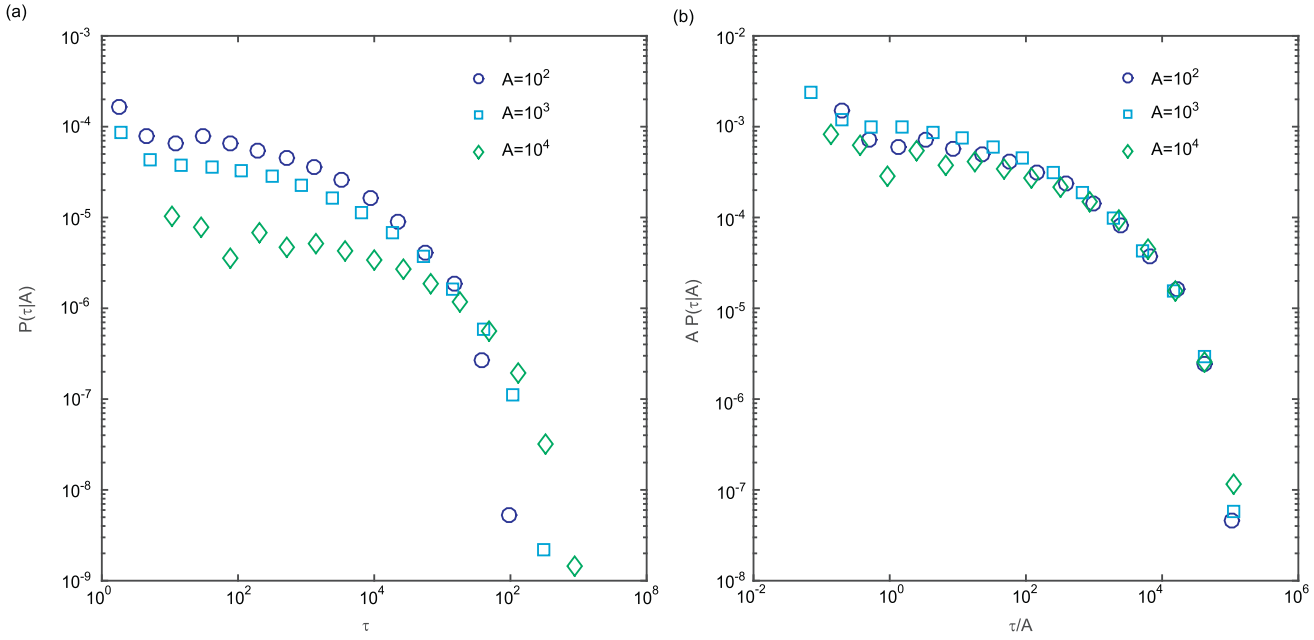

Fig. B.12. Persistence time distributions for the N-SI model. Colors refer to different values of A. (a) $p(\tau|A)$ for the N-SI model with $\lambda = 10^{-3}$ and $A = 10^i$ with $i = 2, 3, 4$. (b) $Ap(\tau|A)$ is a function of τ/A^z, where z is the SAR exponent (see text).

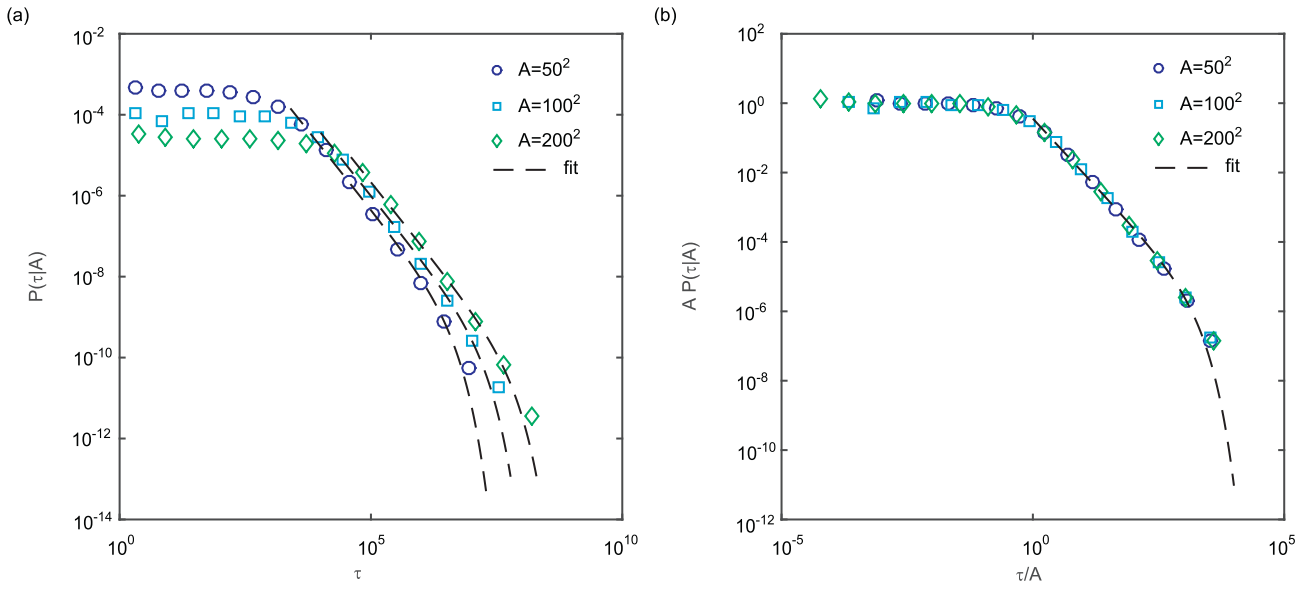

Fig. B.13. Persistence-time distribution for the MSV model. (a) $p(\tau|A)$ for the MSV model with $\lambda = 10^{-3}$ and $A = L^2$ with $L = 50, 100, 200$. The dotted lines are maximum likelihood fits of the tail of the distribution ($\tau > A$) to a power-function with exponential cutoff (Eq. (B.3)). (b) $Ap(\tau|A)$ is a function of τ/A (see text).

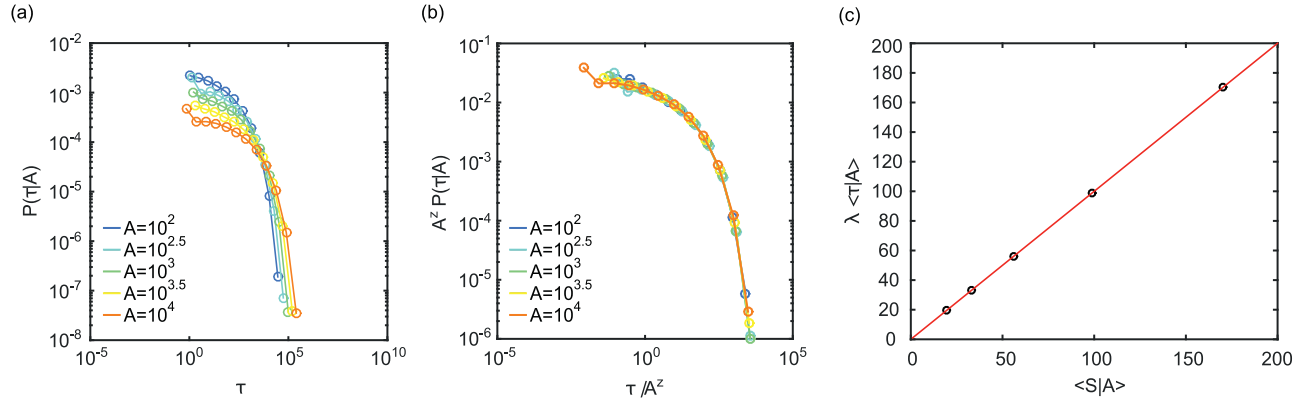

Fig. B.14. Persistence time distributions for model M1. (a) $p(\tau|A)$, colors from blue to orange correspond to areas $A = 10^i$ with $i = 2, 2.5, 3, 3.5, 4$. (b) $Ap(\tau|A)$ is a function of τ/A^z, where z is the SAR exponent (see text). (c) Plot of $\langle S|A\rangle$, vs $\lambda\langle\tau|A\rangle$, showing that Eq. (5) of the main text is verified. The continuous line has slope one. (For interpretation of the references to colour in this figure legend, the reader is referred to the web version of this article.)

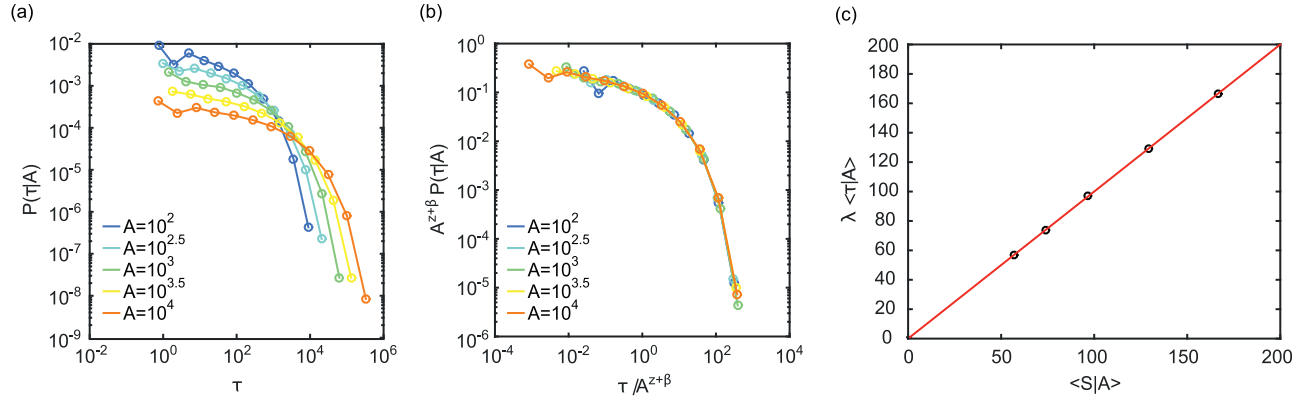

Fig. B.15. Persistence time distribution for model M2. (a) $p(\tau|A)$, colors from blue to orange correspond to areas $A = 10^i$ with $i = 2, 2.5, 3, 3.5, 4$. (b) $Ap(\tau|A)$ is a function of $\tau/A^{z+\beta}$, where z is the SAR exponent and β the exponent of the dependence of the diversification rate on A (see text). (c) Plot of $\langle S|A\rangle$, vs $\lambda\langle\tau|A\rangle$, showing that Eq. (5) of the main text is verified. The continuous line has slope one. (For interpretation of the references to colour in this figure legend, the reader is referred to the web version of this article.)

Appendix C. $p(S|A)$ in non-neutral models

Let $p(S|A)$ be the probability that in a patch of area A, at stationarity, S species coexist. From the numerical implementations of our non-neutral models of community dynamics, we found that $p(S|A)$ satisfies:

$$p(S|A) = \frac{\mathcal{C}}{S}\tilde{\mathcal{F}}\left(\frac{S}{cA^z}\right) \tag{C.1}$$

where $\tilde{\mathcal{F}}$ is a function such that $\tilde{\mathcal{F}}(x) \to 0$ when $x \to 0, \infty$, $\mathcal{C}$ is a normalization constant and for the purpose of this section we consider c to be constant (and thus we ignore the conditional dependency of $p(S|A)$ on c in this section). To compute the normalization constant and the moments, we will treat S as a continuous variable, approximating sums over $S = 1, 2, .$ with integrals over $[0, \infty)$. When $A \gg 1$, this is a good approximation thanks to the behavior of the function $\mathcal{F}(x)$ in $x \sim 0$. In fact, in the region $S \sim 1$, where the integral and the sum would differ, contributions are negligible if $\mathcal{F}(x)$ goes to 0 fast enough, which is verified in our models. Normalization imposes the following constraint:

$$1 = \int_0^\infty p(S|A)dS = \mathcal{C}\int_0^\infty \frac{1}{S}\tilde{\mathcal{F}}\left(\frac{S}{cA^z}\right)dS = \mathcal{C}\int_0^\infty \frac{1}{x}\tilde{\mathcal{F}}(x)dx, \tag{C.2}$$

where we performed the change of variables $x = S/(cA^z)$. Correctly, the normalization constant does not depend on A, and it is given by $\mathcal{C} = 1/\int_0^\infty x^{-1}\tilde{\mathcal{F}}(x)dx$. Finally,

$$p(S|A) = \frac{1}{S}\mathcal{F}\left(\frac{S}{cA^z}\right) \tag{C.3}$$

where we defined $\mathcal{F}(x) := \tilde{\mathcal{F}}(x)/\mathcal{C}$. The moments of $p(S|A)$ are obtained as

$$\begin{aligned}\langle S^i|A\rangle &= \int_0^\infty S^i p(S|A)dS \\ &= \int_0^\infty S^{i-1}\mathcal{F}\left(\frac{S}{cA^z}\right)dS \propto A^{zi}\int_0^\infty x^{i-1}\mathcal{F}(x)dx \propto A^{zi}.\end{aligned} \tag{C.4}$$

This implies that the SAR is a power-law, $\langle S|A\rangle \propto A^z$, and that the ratio of consecutive moments satisfies

$$\frac{\langle S^{i+1}|A\rangle}{\langle S^i|A\rangle} \propto A^z \propto \langle S|A\rangle. \tag{C.5}$$

Appendix D. Deterministic community dynamics model of a community subject to periodic perturbations

In this section, we study a deterministic model describing the dynamics of the number of species S in a community subject to periodical perturbations causing the extinction of species. The model is intended to mimic the stochastic community dynamics models N-SI-P1 and N-SI-P2 in a simplified way which allows us to obtain analytic results explaining qualitatively the behavior of the two stochastic community dynamics models. As we will see, this is possible only if the perturbations dominate over intrinsic stochasticity in determining the statistics of S.

Let ν_p be the frequency of perturbations and fS^α the number of species going extinct due to a perturbation, where S is the number of species present at the moment when the perturbation occurs and $\alpha \in [0, 1]$. The values $\alpha = 0, 1$ correspond, respectively, to the situations in models N-SI-P1 and N-SI-P2. We assume, for simplicity, that S grows linearly with rate s between two perturbations, but analogous computations can be performed also for other types of growth. The stationary value of S in the unperturbed N-SI model, $\bar{S}_{st} = cA^z$, is taken as a hard boundary to the growth of S. Here, we neglect habitat heterogeneity across different patches and thus we set $c = 1$. Supposing that the upper boundary $\bar{S}_{st}$ was reached before a perturbation, the time T needed to return to it satisfies:

$$A^z - fA^{\alpha z} + sT = A^z, \tag{D.1}$$

therefore $T = fA^{\alpha z}/s$. We must therefore distinguish two cases: i) when $T \leq 1/\nu$, the upper boundary is reached between two perturbations, and the number of species in the community remains at $S = \bar{S}_{st}$ for an interval $1/\nu - T$ (see Fig. D.16(a)); ii) when $T > 1/\nu$ the upper boundary is never reached, and the community eventually stabilizes on a cycle in which the increase in the number of species in time $1/\nu$ is equal to the loss of species due to the perturbation (see Fig. D.16(b)). Defining $\eta = \nu f A^{\alpha z}/s$, the two cases are identified by $\eta \leq 1$ and $\eta > 1$. Note that, when $\alpha = 0$, η does not depend on A. Therefore, all other parameter being fixed, communities in patches of different size A all belong to the same case: either they all reach the upper boundary of S, or none of them does.

Case $\eta \leq 1$

After an initial phase in which there is net growth, the upper boundary is reached and $S(t)$ becomes periodic with period $1/\nu$. Within a period, the evolution of S is described by

$$S(t) = \begin{cases} A^z - fA^{\alpha z} + st & t \leq T \\ A^z & t > T. \end{cases} \tag{D.2}$$

We can compute the average of S over a period as follows:

$$\begin{aligned}\langle S|A\rangle &= \nu\int_0^{1/\nu} S(t)dt = \nu\left[\int_0^T (A^z - fA^{\alpha z} + st)dt + \int_T^{1/\nu} A^z dt\right] \\ &= A^z\left(1 - \frac{\eta f}{2}A^{-(1-\alpha)z}\right).\end{aligned} \tag{D.3}$$

One immediately sees that, for $\eta \ll 1$, the SAR is a power-law with slope z. For non-negligible η values, the slope of the SAR is obtained as

$$\frac{d\log\langle S|A\rangle}{d\log A} = z\left(1 - \frac{2\alpha - 1}{\frac{2s}{f^2\nu A^{2\alpha-1}} - 1}\right). \tag{D.4}$$

Therefore, when $\alpha > 1/2$ the slope changes from z to 0 as A increases (all other parameters being equal, valid until $\eta \leq 1$). When $\alpha < 1/2$, instead, the slope is z in the large A limit. This result explains why model N-SI-P1 has a power-law SAR similar to the one in the absence of perturbations, while the N-SI-P2 model has a SAR with gradually decreasing slope. The plateau reached at larger areas for model N-SI-P2 is explained by the case $\eta > 1$.

To compute the exponent β, we first compute the second moment of S:

$$\begin{aligned}\langle S^2|A\rangle &= \nu\int_0^{1/\nu} S(t)^2 dt = \nu\left[\int_0^T (A^z - fA^{\alpha z} + st)^2 dt + \int_T^{1/\nu} A^{2z}dt\right] \\ &= A^{2z} - f\eta A^{(\alpha+1)z} + \frac{f^2\eta}{3}A^{2\alpha z}.\end{aligned} \tag{D.5}$$

Therefore, we have

$$\begin{aligned}\mathrm{var}(S|A) &= \langle S^2|A\rangle - \langle S|A\rangle^2 = A^{2\alpha z}\frac{f^2\eta}{3}\left(1 - \frac{3}{4}\eta\right) \\ &= A^{3\alpha z}\frac{f^3\nu}{3s}\left(1 - \frac{3}{4}\eta\right),\end{aligned} \tag{D.6}$$

which, when $\eta \ll 1$, gives $\beta = 3\alpha$. For $\alpha = 1$, this explains correctly the results of model N-SI-P2 for intermediate values of the area. For $\alpha = 1/3$ the fluctuations given by the perturbations are characterized by $\beta = 1$, therefore they have the same scaling as the fluctuations due to the intrinsic stochasticity of the dynamics. For $\alpha < 1/3$, therefore, the predictions of the deterministic model are not valid, because the intrinsic stochasticity will dominate on the perturbations, giving $\beta = 1$, as observed for the N-SI-P1 model ($\alpha = 0$).

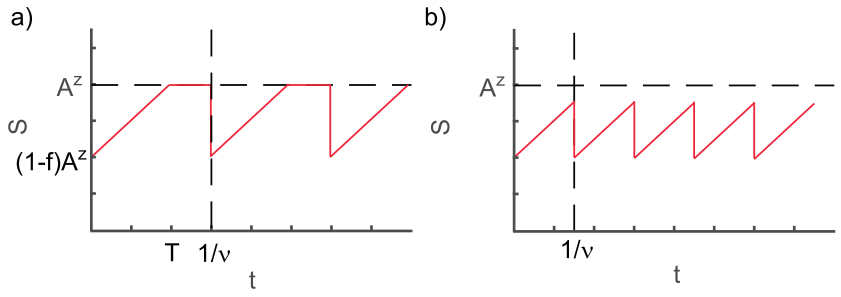

Fig. D.16. Dynamics of the deterministic model of a community subject to perturbations described in Section 2.4. (a) Case $\eta \leq 1$, the number of species in the community reaches the upper boundary; (b) case $\eta > 1$, the number of species in the community never reaches the upper boundary.

Case $\eta > 1$

When $\eta > 1$, the dynamics of S becomes periodical before reaching the upper boundary $S = A^z$. To show this, let us consider the case $\alpha = 1$ for simplicity and call S_i the number of species after the i-th perturbation. The dynamics is therefore expressed by:

$$S_{i+1} = \min\{(1-f)(S_i + s/\nu), (1-f)A^z\}. \tag{D.7}$$

This process has two fixed points, $\tilde{S}_1 = (1-f)s/(\nu f)$ and $\tilde{S}_2 = (1-f)A^z$. The fixed point $\tilde{S}_1$, corresponding to the situation in which the growth in an interval of length $1/\nu$ is equaled by the loss of species due to a perturbation, is attractive, i.e. $|\tilde{S}_1 - S_{i+1}| < |\tilde{S}_1 - S_i|$. Therefore, when $\tilde{S}_1 < \tilde{S}_2$ (which is, when $\eta > 1$), the process will tend to this fixed point $\forall S_0 < A^z$. This situation corresponds to a periodic dynamics described by

$$S(t) = \frac{(1-f)s}{\nu f} + st \qquad t \leq 1/\nu \tag{D.8}$$

which does not depend on A. The average over a period therefore is also independent of A:

$$\langle S|A\rangle = \langle S\rangle = \nu \int_0^{1/\nu} S(t) = \frac{s(2-f)}{2\nu f}, \tag{D.9}$$

which explains the plateau observed in the SAR of model N-SI-P2 in Fig. 10. Being $S(t)$ independent of A, all moments are independent of A and therefore also the coefficient of variation CV(S) is constant.

References

Arrhenius, O., 1921. Species and area. J. Ecol. 9, 95–99.

Azaele, S., Suweis, S., Grilli, J., Volkov, I., Banavar, J.R., Maritan, A., 2016. Statistical mechanics of ecological systems: neutral theory and beyond. Rev. Mod. Phys. 88, 035003. doi:10.1103/RevModPhys.88.035003.

Banavar, J., Damuth, J., Maritan, A., Rinaldo, A., 2007. Scaling in ecosystems and the linkage of macroecological laws. Phys. Rev. Lett. 98 (1), 068104.

Bellin, A., Rubin, Y., 1996. HYDRO_GEN: A spatially distributed random field generator for correlated properties. Stochastic Hydrol. Hydraulics 10, 253–278. doi:10.1007/BF01581869.

Benes, V.E., 1965. Mathematical theory of connecting network and telephon traffic. Academic Press, New York and London.

Bertuzzo, E., Rodriguez-Iturbe, I., Rinaldo, A., 2015. Metapopulation capacity of evolving fluvial landscapes. Water Resour. Res. 51 (4), 2696–2706. doi:10.1002/2015WR016946.

Bertuzzo, E., Suweis, S., Mari, L., Maritan, A., Rodriguez-Iturbe, I., Rinaldo, A., 2011. Spatial effects for species persistence and implications for biodiversity. Proc. Natl. Acad. Sci. USA 108 (11), 4346–4351.

Bhattacharjee, S.M., Seno, F., 2001. A measure of data collapse for scaling. J. Phys. A Math. Gen. 34 (33), 6375–6380.

Borile, C., Maritan, A., Munoz, M., 2013. The effect of quenched disorder in neutral theories. J. Stat. Mech 4, p04032.

Brown, J.H., Gillooly, J.F., Allen, A.P., Savage, V.M., West, G.B., 2004. Toward a metabolic theory of ecology. Ecology 85 (7), 1771–1789. doi:10.1890/03-9000.

Cencini, M., Pigolotti, S., Munoz, M., 2012. What ecological factors shape species-area curves in neutral models? PLoS ONE 7 (6), e38232. doi:10.1371/journal.pone.0038232.

Chisholm, R.A., Lichstein, J.W., 2009. Linking dispersal, immigration and scale in the neutral theory of biodiversity. Ecol. Lett. 12 (12), 1385–1393. doi:10.1111/j.1461-0248.2009.01389.x.

Clifford, P., Aidan, W.S., 1973. A model for spatial conflict. Biometrika 60 (3), 581–588. doi:10.2307/2335008.

Cohen, J., 2014. Stochastic population dynamics in a Markovian environment implies Taylor's power law of fluctuation scaling. Theor. Ecol. 7, 77–86.

Damuth, J., 1981. Population density and body size in mammals. Nature 290, 699–700.

Dengler, J., 2009. Which function describes the species area relationship best? a review and empirical evaluation. J. Biogeogr. 36 (4), 728–744. doi:10.1111/j.1365-2699.2008.02038.x.

Diamond, J.M., Gilpin, M.E., 1980. Turnover noise: contribution to variance in species number and prediction from immigration and extinction curves. Am. Nat. 115 (6), 884–889. doi:10.1086/283607.

Didier, S., Rama, C., 1997. Convergent multiplicative processes repelled from zero: power laws and truncated power laws. J. Phys. I France 7 (3), 431–444. doi:10.1051/jp1:1997169.

Dornelas, M., Gotelli, N.J., McGill, B., Shimadzu, H., Moyes, F., Sievers, C., Magurran, A.E., 2014. Assemblage time series reveal biodiversity change but not systematic loss. Science 344 (6181), 296–299. doi:10.1126/science.1248484.

Drakare, S., Lennon, J., Hillebrand, H., 2006. The imprint of the geographical, evolutionary and ecological context on species–area relationships. Ecol. Lett. 9, 215–227.

Durrett, R., Levin, S., 1996. Spatial models for species-area curves. J. Theor. Biol. 179 (2), 119–127. doi:10.1006/jtbi.1996.0053.

Etienne, R.S., Olff, H., 2004. A novel genealogical approach to neutral biodiversity theory. Ecol. Lett. 7 (3), 170–175. doi:10.1111/j.1461-0248.2004.00572.x.

Giometto, A., Altermatt, F., Carrara, F., Maritan, A., Rinaldo, A., 2013. Scaling body size fluctuations. Proc. Natl. Acad. Sci. U.S.A. 110 (12), 4646–4650. doi:10.1073/pnas.1301552110.

Giometto, A., Formentin, M., Rinaldo, A., Cohen, J., Maritan, A., 2015. Sample and population exponents of generalized taylor's law. Proc. Natl. Acad. Sci. USA 112 (25), 7755–7760.

Gleason, H., 1922. On the relation between species and area. Ecology 3, 156–162.

Grilli, J., Barabas, G., Allesina, S., 2015. Metapopulation persistence in random fragmented landscapes. PLoS Comput. Biol. 11, e100251.

Hanski, I., 1998. Metapopulation dynamics. Nature 396, 41–49.

Hanski, I., Ovaskainen, O., 2000. The metapopulation capacity of a fragmented landscape. Nature 404 (6779), 755–758. doi:10.1038/35008063.

Hanski, I., Zurita, G., Bellocq, M., Rybicki, J., 2013. Species-fragmented area relationship. Proc. Natl. Acad. Sci. USA 110, 12715–12720.

Harte, J., Smith, A., Storch, D., 2009. Biodiversity scales from plots to biomes with a universal species–area curve. Ecol. Lett. 12, 789–797.

Holley, R., Liggett, T., 1975. Ergodic theorems for weakly interacting infinite systems and the voter model. Ann. Probab. 3 (4), 643–663.

Hubbell, S., 2001. The unified theory of biodiversity and biogeography. Princeton Univ. Press, Princeton.

Kleiber, 1932. Body size and metabolism. Hilgardia 6 (11), 315–353.

Levin, S., 1992. The problem of pattern and scale in ecology. Ecology 76, 1943–1963.

Liggett, T.M., 1985. Interacting particle systems. Springer Verlag, New York.

Lomolino, M., 2000. Ecology's most general, yet protean pattern: the species–area relationship. J. Biogeogr. 27 (12), 17–26.

Losos, J., Schluter, D., 2000. Analysis of an evolutionary species-area relationship. Nature 408 (6814), 847–850.

MacArthur, M., Wilson, E., 1963. An equilibrium theory of insular zoogeography. Evolution 17, 373–387.

MacArthur, M., Wilson, E., 1967. The theory of island biogeography. Princeton Univ. Press, Princeton.

Marañón, E., 2015. Cell size as a key determinant of phytoplankton metabolism and community structure. Ann. Rev. Mar. Sci. 7 (1), 241–264. doi:10.1146/annurev-marine-010814-015955.

Marquet, P.A., Quiñones, R.A., Abades, S., Labra, F., Tognelli, M., Arim, M., Rivadeneira, M., 2005. Scaling and power-laws in ecological systems. J. Exp. Biol. 208, 1749–1769. doi:10.1242/jeb.01588.

Newman, M., 2005. Power laws, pareto distributions and zipf's law. Contemp. Phys. 46 (5), 323–351.
Pigolotti, S., Cencini, M., 2009. Speciation-rate dependence in species–area relationships. J. Theor. Biol. 260 (1), 83–89. doi:10.1016/j.jtbi.2009.05.023.
Pimm, S., Raven, P., 1995. Biodiversity – extinction by numbers. Nature 403, 843–845.
Rosenzweig, M., 1995. Species diversity in space and time. Cambridge Univ. Press, New York.
Rosindell, J., Cornell, S., 2009. Species-area curves, neutral models and long-distance dispersal. Ecology 90, 1743–1750.
Rosindell, J., Wong, Y., Etienne, R., 2008. A coalescence approach to spatial neutral ecology. Ecol. Inform. 3 (3), 259–271. doi:10.1016/j.ecoinf.2008.05.001.
Rybicki, J., Hanski, I., 2013. Species-area relationships and extinctions caused by habitat loss and fragmentation. Ecol. Lett. 16 (1), 27–38.
Schluter, D., Pennell, M., 2017. Speciation gradients and the distribution of biodiversity. Nature 546, 48–55.
Shem-Tov, Y., Danino, M., Shnerb, N.M., 2017. Solution of the spatial neutral model yields new bounds on the Amazonian species richness. Sci. Rep. 7, 42415.
Solomon, S., Levy, M., 1996. Spontaneous scaling emergence in generic stochastic systems. Int. J. Mod. Phys. C 07 (05), 745–751. doi:10.1142/S0129183196000624.
Suweis, S., Rinaldo, A., Maritan, A., 2012. An exactly solvable coarse-grained model for species diversity. J. Stat. Mech. Theory Exp. 2012 (07), P07017. doi:10.1088/1742-5468/2012/07/P07017.
Taylor, L.R., 1961. Aggregation, variance and the mean. Nature 189 (4766), 732–735.
Thomas, C., Cameron, A., Green, R., Bakkenes, M., Beaumont, L., Collingham, Y.E., 2004. Extinction risk from climate change. Nature 427, 145–148.
Triantis, K., Guilhaumon, F., Whittaker, R., 2012. The island species–area relationship: biology and statistics. J. Biogeogr. 39 (2), 215–231. doi:10.1111/j.1365-2699.2011.02652.x.
Vellend, M., Baeten, L., Myers-Smith, I.H., Elmendorf, S.C., Beauséjour, R., Brown, C.D., De Frenne, P., Verheyen, K., Wipf, S., 2013. Global meta-analysis reveals no net change in local-scale plant biodiversity over time. Proc. Natl. Acad. Sci. 110 (48), 19456–19459. doi:10.1073/pnas.1312779110.
Wagner, C., Harmon, L., Seehausen, O., 2014. Cichlid species-area relationships are shaped by adaptive radiations that scale with area. Ecol. Lett. 17 (5), 583–592.
Zaoli, S., Giometto, A., Maritan, A., Rinaldo, A., 2017. Covariations in ecological scaling laws fostered by community dynamics. Proc. Natl Acad. Sci. USA 114, 10672–10677. doi:10.1073/pnas.1708376114.